

# Dry Periods Amplify the Amazon and Congo Forests' Rainfall Self-Reliance

Lan Wang-Erlandsson<sup>1</sup>, Ruud J. van der Ent<sup>2</sup>, Arie Staal<sup>3</sup>, Patrick Keys<sup>4</sup>, Delphine Clara Zemp<sup>5</sup>, Ingo Fetzer<sup>1</sup>, Makoto Taniguchi<sup>6</sup>, and Line Gordon<sup>1</sup>

<sup>1</sup>Stockholm Resilience Centre, Stockholm University

<sup>2</sup>Delft University of Technology

<sup>3</sup>Utrecht University

<sup>4</sup>Department of Atmospheric Science, Colorado State University

<sup>5</sup>University of Neuchâtel

<sup>6</sup>Research Institute for Humanity and Nature

April 3, 2023

## Abstract

A substantial amount of the tropical forests of South America and Africa is generated through moisture recycling (i.e., forest rainfall self-reliance). Thus, deforestation that reduces evaporation and dampens the water cycle can further increase the risk of water-stress-induced forest loss in downwind areas, particularly during water scarce periods. However, few studies have investigated dry period forest rainfall self-reliance over longer records and consistently compared the rainforest moisture recycling in both continents. Here, we analyze dry-season anomalies of moisture recycling for mean-years and dry-years, in the South American (Amazon) and African (Congo) rainforests over the years 1980-2013. We find that, in the dry seasons, the reliance of forest rainfall on their own moisture supply ( $\rho_{for}$ ) increases by 7% (from a mean annual value of 26% to 28%) in the Amazon and up to 30% (from 28% to 36%) in the Congo. Dry years further amplify dry season  $\rho_{for}$  in both regions by 4-5%. In both the Amazon and Congo, dry season amplification of  $\rho_{for}$  is strongest in regions with a high mean annual  $\rho_{for}$ . In the Amazon, forest rainfall self-reliance has declined over time. At the country scale, dry season  $\rho_{for}$  can differ drastically from mean annual  $\rho_{for}$ . In for example Bolivia and Gabon, mean annual  $\rho_{for}$  is  $\sim$ 30% while dry season  $\rho_{for}$  is  $\sim$ 50%. The dry period amplification of forest rainfall self-reliance further highlights the role of forests for sustaining their own resilience, and for maintaining downwind rainfall at both regional and national scales.

## Hosted file

958625\_0\_art\_file\_10833069\_rs2qg3.docx available at <https://authorea.com/users/308363/articles/632823-dry-periods-amplify-the-amazon-and-congo-forests-rainfall-self-reliance>

## Hosted file

958625\_0\_supp\_10797917\_rr4sv4.docx available at <https://authorea.com/users/308363/articles/632823-dry-periods-amplify-the-amazon-and-congo-forests-rainfall-self-reliance>

1  
2  
3  
4  
5  
6  
7  
8  
9  
10  
11  
12  
13  
14  
15  
16  
17  
18  
19  
20  
21  
22

## **Dry Periods Amplify the Amazon and Congo Forests' Rainfall Self-Reliance**

**Lan Wang-Erlandsson<sup>1,2,3,4</sup>, Ruud van der Ent<sup>5</sup>, Arie Staal<sup>1,6</sup>, Patrick Keys<sup>7</sup>, Delphine Clara Zemp<sup>8</sup>, Ingo Fetzer<sup>1,2,4</sup>, Makoto Taniguchi<sup>3</sup>, and Line J. Gordon<sup>1</sup>**

<sup>1</sup>Stockholm Resilience Centre (SRC), Stockholm University, Sweden.

<sup>2</sup>Bolin Centre for Climate Research, Stockholm University, Sweden.

<sup>3</sup>Research Institute for Humanity and Nature (RIHN), Japan.

<sup>4</sup>Potsdam Institute for Climate Impact Research (PIK), Member of the Leibniz Association, Germany.

<sup>5</sup>Department of Water Management, Delft University of Technology, the Netherlands.

<sup>6</sup>Copernicus Institute of Sustainable Development, Utrecht University, the Netherlands.

<sup>7</sup>Department of Atmospheric Science, Colorado State University, USA.

<sup>8</sup>University of Neuchâtel, Switzerland.

Corresponding author: Lan Wang-Erlandsson ([lan.wang@su.se](mailto:lan.wang@su.se))

### **Key Points:**

- In South America, and particularly Africa, the share of forest rainfall that originates from the forest itself is higher in dry seasons.
- Dry years further amplify rainfall self-reliance.
- Several countries in Africa receive up to half of their rainfall from rainforests during dry seasons and dry years.

**Abstract**

A substantial amount of the tropical forests of South America and Africa is generated through moisture recycling (i.e., forest rainfall self-reliance). Thus, deforestation that reduces evaporation and dampens the water cycle can further increase the risk of water-stress-induced forest loss in downwind areas, particularly during water scarce periods. However, few studies have investigated dry period forest rainfall self-reliance over longer records and consistently compared the rainforest moisture recycling in both continents. Here, we analyze dry-season anomalies of moisture recycling for mean-years and dry-years, in the South American (Amazon) and African (Congo) rainforests over the years 1980-2013. We find that, in the dry seasons, the reliance of forest rainfall on their own moisture supply ( $\rho_{\text{for}}$ ) increases by 7% (from a mean annual value of 26% to 28%) in the Amazon and up to 30% (from 28% to 36%) in the Congo. Dry years further amplify dry season  $\rho_{\text{for}}$  in both regions by 4-5%. In both the Amazon and Congo, dry season amplification of  $\rho_{\text{for}}$  is strongest in regions with a high mean annual  $\rho_{\text{for}}$ . In the Amazon, forest rainfall self-reliance has declined over time. At the country scale, dry season  $\rho_{\text{for}}$  can differ drastically from mean annual  $\rho_{\text{for}}$ . In for example Bolivia and Gabon, mean annual  $\rho_{\text{for}}$  is ~30% while dry season  $\rho_{\text{for}}$  is ~50%. The dry period amplification of forest rainfall self-reliance further highlights the role of forests for sustaining their own resilience, and for maintaining downwind rainfall at both regional and national scales.

41

**Plain Language Summary**

A substantial amount of the rainfall over the South American and African tropical rainforest originate from moisture generated by the forests themselves. Therefore, forest loss can reduce rainfall and lead to water stress in downwind areas. Few studies have analyzed and compared how the two rainforests contribute to their own rainfall during dry periods. In this study, we

46

47 analyzed three decades of data and found that a larger fraction of the rainfall over forests is  
48 generated by the forests themselves during dry periods than usual. Thus, rainforests are  
49 particularly important for the generation of its own rainfall, when rainfall levels are already low  
50 and when the rainforests are potentially most vulnerable to droughts. The degree of reliance of  
51 rainforest rainfall on its own moisture amplifies by 7% in the rainforests of South America, 30%  
52 in the African rainforests in dry seasons, and more during dry seasons in dry years. Locally, the  
53 amplification can be even stronger, particularly in areas where the rainfall self-reliance is already  
54 high under usual climate conditions. The dry period amplification of forest rainfall self-reliance  
55 underscores the importance of preserving forests in order to maintain water availability in the  
56 forests themselves and in downwind regions.

## 57 **1 Introduction**

58 The tropical rainforests of the Amazon and Congo are hotspots of global biodiversity (Pimm et  
59 al., 2014) and critical for the global carbon cycle (Hubau et al., 2020; Mitchard, 2018). However,  
60 deforestation is increasing (Silva Junior et al., 2021; Tchatchou, Sonwa, Anne, & Tiani, 2015)  
61 along with aridity and droughts over both regions (Dai, 2013; Duffy, Brando, Asner, & Field,  
62 2015; Zhou et al., 2014). The drier hydroclimate negatively influences forest functioning (e.g.,  
63 carbon sequestration and storage) and resilience, i.e., the forest ecosystem's ability to absorb or  
64 withstand perturbations (Boulton, Lenton, & Boers, 2022; Forzieri, Dakos, Mcdowell, Ramdane,  
65 & Cescatti, 2022; Lewis, Edwards, & Galbraith, 2015; Malhi, Gardner, Goldsmith, Silman, &  
66 Zelazowski, 2014). Remote-sensing-based studies indicate that rainfall constitutes a key variable  
67 in determining the risk for forest-to-savanna transitions (Hirota, Holmgren, van Nes, & Scheffer,  
68 2011; Staver, Archibald, & Levin, 2011).

69 Forest loss affects forest functioning and resilience directly, but also indirectly by  
70 reducing evaporation and subsequent rainfall through the perturbation of the water balance.  
71 Namely, the return of terrestrial evaporation as precipitation over land areas, termed *terrestrial*  
72 *moisture recycling*, allows evaporation change to cascade across the continents (Zemp et al.,  
73 2017). Atmospheric moisture tracking, based on e.g., water balance and data on atmospheric  
74 humidity, wind speed, evaporation, and precipitation, allows us to map and analyze the  
75 evaporative source of precipitation (i.e., moisture sources), and where evaporation falls out as  
76 precipitation (i.e., moisture sinks) (Keys et al., 2012; O. A. Tuinenburg & Staal, 2020; van der  
77 Ent, Savenije, Schaefli, & Steele-Dunne, 2010).

78 In parts of the Amazon and Congo rainforests, the percentage of precipitation from land  
79 can be up to 60-80%, i.e. the majority of the mean annual rainfall originates from terrestrial  
80 evaporation (Dominguez et al., 2022; Dyer et al., 2017; Spracklen, Arnold, & Taylor, 2012;  
81 Spracklen & Garcia-Carreras, 2015; van der Ent et al., 2010). This can be both a boon and a bane  
82 for forest resilience: retained vegetation transpiration helps to buffer against droughts by  
83 providing moisture for subsequent rainfall (Staal et al., 2018), while long-term moisture flow  
84 disruptions can lead to self-amplified forest loss (Wunderling et al., 2022; Zemp et al., 2017).  
85 Thus, where increased reliance of precipitation on forest moisture supply coincides with dry  
86 periods, it may enable both regional and global-scale self-reinforcing feedbacks between forest  
87 loss and drier conditions (Staal et al., 2020; Zemp et al., 2017). In the Amazon, stronger regional  
88 forest-rainfall relationships during dry periods have been suggested to increase the negative  
89 effects of deforestation for forest resilience (Bagley, Desai, Harding, Snyder, & Foley, 2014;  
90 Staal et al., 2018) and agriculture production (Leite-Filho, Soares-filho, Davis, Abrahão, &  
91 Börner, 2021). Further, due to a nonlinear relationship between atmospheric moisture content

92 and rainfall, minor decrease in moisture content could reduce rainfall drastically (Baudena,  
93 Tuinenburg, Ferdinand, & Staal, 2021). However, studies have contrasting conclusions for  
94 temporal variations of the extent that rainforests depend on their own moisture supply for  
95 rainfall, which may be explained by differences in study region selection, methods, assumptions  
96 and time period considered (overview in Table S2 and S3).

97 In the Amazon, some atmospheric moisture studies suggest that forest rainfall self-  
98 reliance is highest in the dry season (Angelini et al., 2011; Burde, Gandush, & Bayarjargal, 2006;  
99 Eltahir & Bras, 1994; Staal et al., 2018; Zemp et al., 2014), while others suggest the wet season  
100 (Burde et al., 2006; Satyamurty, da Costa, & Manzi, 2013). Consistent with a higher rainfall self-  
101 reliance during the dry season, Spracklen et al., (2012) showed that deforestation leads to a larger  
102 rainfall reduction in the dry season (-21% change) than in the wet season (-12% change). Dry  
103 season rainfall self-reliance (in percent) has been shown to be about 7% higher during the two  
104 mega-drought years 2005 and 2010 relative to wet years (Bagley et al., 2014). Such dry-year dry-  
105 season anomaly are important to understand as any marginal increase in water deficit during the  
106 dry season can have a large impact, e.g., on streamflow and carbon balance (Marengo,  
107 Tomasella, Alves, Soares, & Rodriguez, 2011; Mitchard, 2018).

108 Estimates of rainfall self-reliance also vary in the Congo. Pokam, Djiotang, & Mkankam  
109 (2012) report the highest ratios during both dry seasons December-January-February and June-  
110 July-August for a rectangular region mostly over the forested regions. Dyer et al., (2017), who  
111 selected a rectangular region over the basin, observed the highest ratio during the June-July-  
112 August dry season, but below-average ratios during the other dry season December-January-  
113 February. In contrast, Sorí, Nieto, Vicente-Serrano, Drumond, & Gimeno (2017), who used the  
114 actual basin delineation, suggest that basin rainfall self-reliance are the highest in the rainy

115 season, and below average in the dry season month July. (Sorí et al., 2017)(Sorí et al., 2017)(Sorí  
116 et al., 2017)(Sorí et al., 2017)(Sorí et al., 2017)While discrepancies remain regarding the spatio-  
117 temporal variability of continental moisture recycling in the Congo, higher rainfall dependency  
118 on terrestrial evaporation sources in dry seasons is also indicated by isotope studies (Worden, Fu,  
119 Chakraborty, Liu, & Worden, 2021).

120 Previous studies suggest that increased forest rainfall self-reliance during dry periods  
121 may be associated with reduced oceanic moisture inflow, and increased forest transpiration due  
122 to higher incoming radiation and forests' ability to store and access subsoil water (Bagley et al.,  
123 2014; Costa et al., 2010; O'Connor et al., 2021; Staal et al., 2018; Zemp et al., 2014). High  
124 evaporation from the Amazon has also been associated with the presence of lower-level jets  
125 during the dry season (Nascimento, Herdies, & De Souza, 2016). Sorí et al. (2017) explains that  
126 the weakening of the Congo basin rainfall self-reliance in dry years is due to vertically integrated  
127 moisture flux divergence that favor moisture export from the basin. However, questions remain  
128 with regard to the respective attribution of moisture recycling anomalies to either anomalies in  
129 wind patterns or evaporation, which for example can be relevant for understanding deforestation  
130 impacts on forest rainfall.

131 Because moisture recycling over the Amazon and Congo is often examined in different  
132 studies with different methodologies, cross-comparisons between the two major rainforest  
133 systems often cannot be easily made. Despite the importance of rainfall for forest functioning  
134 and resilience (e.g. Singh, van der Ent, Wang-Erlandsson, & Fetzer, (2022)), we still have  
135 limited knowledge of how variations in forest self-reliance may potentially interact with dry  
136 periods and deforestation to negatively impact forest rainfall, and how this process might differ  
137 between the Amazon and Congo.

138 This study aims to investigate the importance of the moisture supply from rainforests in  
 139 South America and Africa for their own rainfall during dry periods, i.e., average dry seasons and  
 140 dry seasons in dry years. Based on atmospheric moisture tracking of forest moisture sources and  
 141 sinks over 34 years, we address the following questions: *i.* What are the dry period anomalies of  
 142 forest moisture sources and sinks? (Sect. 4.1, 4.2); *ii.* Are dry period anomalies larger in regions  
 143 with high mean annual forest rainfall self-reliance? (Sect. 4.3); *iii.* To what extent do dry period  
 144 anomalies of forest evaporation contribute to dry period anomalies of forest rainfall self-  
 145 reliance? (Sect. 4.4), and *iv.* How do dry periods affect countries' rainfall reliance on forest  
 146 moisture? (Sect. 4.5).

## 147 2. Materials and methods

### 148 2.1 Moisture recycling model

149 The Eulerian moisture tracking model WAM-2layers (van der Ent, Wang-Erlandsson, Keys, &  
 150 Savenije, 2014) was used to track moisture sources of precipitation and destination of  
 151 evaporation for the Amazon and Congo forest. WAM-2layers tracks atmospheric moisture from  
 152 zero pressure to surface pressure (i.e., from zero pressure at the top of atmosphere to the  
 153 atmospheric pressure at a location on Earth's surface) in two layers. The model applies the water  
 154 balance, and assumes the atmosphere is well mixed within each of the two atmospheric layers.  
 155 To track where evaporation from a given region (source region) falls as precipitation (sink  
 156 region), moisture is tracked forward as follows:

$$157 \frac{\partial S_{\text{tracked}}}{\partial t} = -\frac{\partial(S_{\text{tracked}}u)}{\partial x} - \frac{\partial(S_{\text{tracked}}v)}{\partial y} + E_{\text{tracked}} - P_{\text{tracked}} \pm F_{\text{vertical,tracked}} \quad (1)$$

158 where  $S_{\text{tracked}}$  is the tracked atmospheric storage in an atmospheric column in one layer,  $t$  is time,  
 159  $u$  and  $v$  are wind components in the  $x$  zonal and  $y$  meridional directions,  $E_{\text{tracked}}$  is tracked



160 evaporation entering and  $P_{\text{tracked}}$  is precipitation leaving an atmospheric column in one layer, and  
161  $F_{\text{vertical,tracked}}$  is the tracked vertical moisture transport between the two atmospheric layers.  
162 Evaporation in this paper refers to the total of all types of upward going vapor flows (i.e., ocean  
163 evaporation, transpiration, interception evaporation, soil evaporation, and open water  
164 evaporation) (Miralles, Brutsaert, Dolman, & Gash, 2020), and the terrestrial and forest  
165 evaporation flows that we track naturally preclude the ocean evaporation component. Backward  
166 tracking to determine the source of precipitation uses an analogous equation. We used WAM-  
167 2layers to track moisture for the years 1979-2014, of which 1979 and 2014 were used as spin-up  
168 for the forward and backward tracking, respectively.

169 WAM-2layers has been extensively used to characterize the fate and properties of the  
170 atmospheric branch of the water cycle (e.g., Benedict, van Heerwaarden, van der Linden, Weerts,  
171 & Hazeleger, (2021); Keys et al., (2014); Link, van der Ent, Berger, Eisner, & Finkbeiner,  
172 (2020); van der Ent & Tuinenburg, (2017); Xiao & Cui, (2021)). The moisture tracking  
173 performance generally compares well with Lagrangian type multi-atmospheric-layers moisture  
174 tracking and regional climate model online tracking (van der Ent, Tuinenburg, Knoche,  
175 Kunstmann, & Savenije, 2013), We used a MATLAB version of the model, which is, however,  
176 equivalent in terms of process descriptions as the model used in (van der Ent et al., 2014).

## 177 2.2 Data analyses

178

### 179 2.2.1 Study regions and time periods

180 Moisture tracking was applied to  $1.5^\circ \times 1.5^\circ$  grid cells in South America and Africa with at least  
181 85% tropical evergreen broadleaf forest cover (hereafter referred to as Amazon and Congo  
182 forests). Averaged over the entire study region, each of the two forests has a forest cover of more

183 than 97%. Monthly variations of moisture recycling metrics are shown (in Sect. 4.3) for forest  
 184 moisture source and sink hotspots, here defined as the 25% of the forest grid cells with the  
 185 highest ratios of precipitation from forests and evaporation to forests, respectively.

186 We consider two types of anomalies in this study: (1) the anomaly of dry season in mean  
 187 years compared to mean annual ('dry season anomaly'), and (2) the anomaly of the dry season in  
 188 dry years compared to the dry season in mean years ('dry-year dry-season anomaly'). Based on  
 189 the mean precipitation patterns in the study regions, we select June to September as the dry  
 190 season months for South America, and January-February and June-July-August for Africa, see  
 191 Table S1.

192 We chose to include the six driest years in our analyses, where dryness is defined by the  
 193 intensity of maximum climatological water deficit (MCWD) (years denoted as  $Y_{MCWD}$ ). The  
 194 MCWD captures the drought years well: the three driest years selected here for the Amazon  
 195 (2010, 2005, 1998) based on MCWD also correspond to the three known drought years with  
 196 large effects on forest mortality (Lewis, Brando, Phillips, Heijden, & Nepstad, 2010; Williamson  
 197 et al., 2000), which are associated with warming anomalies of the tropical North Atlantic  
 198 (Marengo et al., 2011).

199 MCWD is defined as the most negative value of climatological water deficit  $C_m$  [mm],  
 200 which is estimated based on monthly precipitation and a fixed reference evaporation rate  $E_{fix}$  at  
 201  $3.3 \text{ mm day}^{-1}$  (used instead of actual  $E$  in order to represent the climatological drought) (Malhi et  
 202 al., 2009; Zemp et al., 2017):

$$203 \quad C_m = \min \left( 0, C_{m-1} + \int_{d_{m,0}}^{d_{m,end}} P_{Y,m} - \int_{d_{m,0}}^{d_{m,end}} E_{fix} \right) \quad (2)$$

204 where  $m$  denotes the month number,  $d_{m,0}$  and  $d_{m,end}$  the first and last day of a month,  $P_{Y,m}$  is the  
 205 precipitation for year  $Y$  and month  $m$ , and  $C_0$  is 0. The climatological water deficit  $C$  is

206 accumulated continuously and reset to zero at the wettest month of the year, at which the next  
 207 12-month period calculation cycle starts (Malhi et al., 2009).

### 208 2.2.2 Moisture recycling analyses and terminology

209 The fraction of rainfall reliance on forest moisture sources  $\rho_{\text{for}}$  [-] (i.e., forest precipitation  
 210 recycling ratio) is defined as:

$$211 \rho_{\text{for}} = P_{\text{for}} / P, \quad (3)$$

212 where  $P_{\text{for}}$  [ $\text{L}^3 \text{ time}^{-1}$  or  $\text{L time}^{-1}$ ] refers to precipitation with forest origin. The  $\rho_{\text{for}}$  are estimated  
 213 for all grid cells globally, and only the  $\rho_{\text{for}}$  values within the forested regions indicate the forest's  
 214 rainfall self-reliance (i.e., the rainforest rainfall reliance on forest moisture sources).

215 The fraction of rainfall reliance on terrestrial moisture sources  $\rho_{\text{terr}}$  [-] (i.e., terrestrial  
 216 precipitation recycling ratio) is similarly defined as

$$217 \rho_{\text{terr}} = P_{\text{terr}} / P, \quad (4)$$

218 where  $P_{\text{terr}}$  [ $\text{L}^3 \text{ time}^{-1}$  or  $\text{L time}^{-1}$ ] denotes precipitation with terrestrial origin at the global scale.

219 The fraction of evaporation that contribute to forest rainfall  $\varepsilon_{\text{for}}$  [-] (i.e., forest evaporation  
 220 recycling ratio) is defined as:

$$221 \varepsilon_{\text{for}} = E_{\text{for}} / E, \quad (5)$$

222 where  $E_{\text{for}}$  [ $\text{L}^3 \text{ time}^{-1}$  or  $\text{L time}^{-1}$ ] refers to evaporation that falls as rainfall in areas with forest  
 223 cover > 85%.

224 Linear trends are calculated by least squares using the Climate Data Toolbox for  
 225 MATLAB (Greene et al., 2019).

226 We analyzed both absolute and relative dry period differences from mean annual or  
 227 seasonal recycling values. The *absolute* dry period recycling anomalies are the difference

228 between dry period and mean years recycling values, e.g., the absolute dry season anomaly of  
 229 terrestrial precipitation recycling ratio is:

$$230 \quad \Delta\rho_{\text{terr,dry-season, abs}} = \rho_{\text{terr,dry-season}} - \rho_{\text{terr,mean-annual}} \quad (6).$$

231 The *relative* dry season recycling anomalies are calculated in relation to the mean annual  
 232 recycling values, e.g., the relative dry season anomaly of terrestrial precipitation recycling ratio  
 233 is:

$$234 \quad \Delta\rho_{\text{terr,dry-season, rel}} = (\rho_{\text{terr,dry-season}} - \rho_{\text{terr,mean-annual}}) / \rho_{\text{terr,mean-annual}} \quad (7).$$

235 Finally, the *relative* dry-year dry-season recycling anomalies are calculated in relation to  
 236 the dry season recycling values, e.g., the relative dry-year dry-season anomaly of terrestrial  
 237 precipitation recycling ratio is:

$$238 \quad \Delta\rho_{\text{terr,dry-year-dry-season, rel}} = (\rho_{\text{terr,dry-year}} - \rho_{\text{terr,dry-season}}) / \rho_{\text{terr,dry-season}} \quad (8).$$

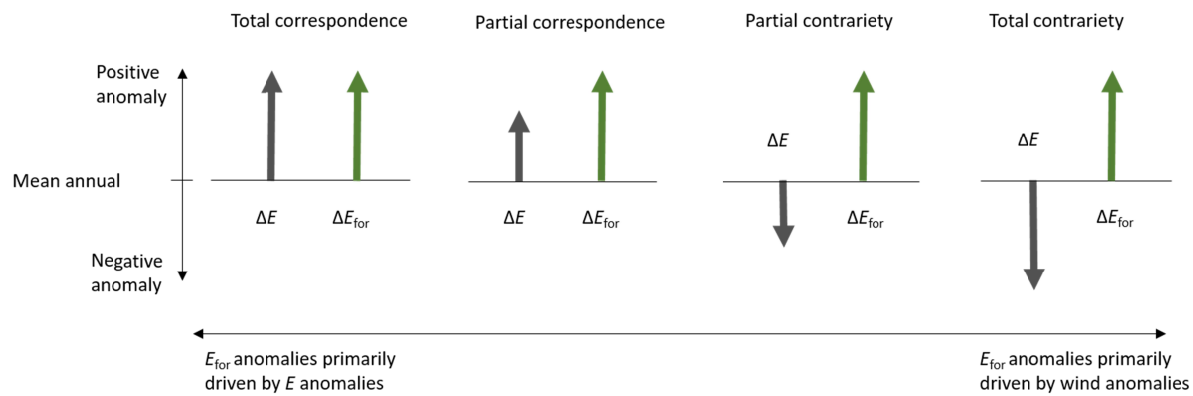
239 2.2.3 Correspondence and contrariety between anomalies of the total evaporation and the  
 240 evaporation that becomes forest rainfall

241 Anomalies of  $E_{\text{for}}$  can be caused by anomalies in  $E$  in source regions and/or by anomalies in  
 242 other meteorological conditions (such as regional wind patterns and rainfall generation in sink  
 243 region). As a means to analyze their respective role of  $E$  contribution to  $E_{\text{for}}$  anomalies, we  
 244 compare the mean absolute volumetric  $E_{\text{for}}$  anomalies with  $E$  anomalies.  $E_{\text{for}}$  anomalies that  
 245 correspond well with  $E$  anomalies can be interpreted as mainly  $E$  driven, whereas contrariety  
 246 shows regions where  $E$  instead buffers against meteorologically driven  $E_{\text{for}}$  anomalies.

247 Each positive and negative  $E_{\text{for}}$  anomaly is comprised of four parts (see example in Figure 1):

- 248 • *total correspondence*, where an  $E$  anomaly agrees in sign with, and is larger than or equal  
 249 to, the  $E_{\text{for}}$  anomaly;

- 250 • *partial correspondence*, where an  $E$  anomaly agrees in sign with, but is smaller than, the  
 251  $E_{\text{for}}$  anomaly;
- 252 • *partial contrariety*, where an  $E$  anomaly disagrees in sign with, and is smaller than, the  
 253  $E_{\text{for}}$  anomaly; and
- 254 • *total contrariety*, where an  $E$  anomaly disagrees in sign with, and is larger than or equal  
 255 to, the  $E_{\text{for}}$  anomaly.



256

257 *Figure 1. Illustration of four categories of the correspondence and contrariety between*  
 258 *anomalies of evaporation ( $\Delta E$ ) and evaporation destined for forest rainfall ( $\Delta E_{\text{for}}$ ). The*  
 259 *conceptual figure illustrates the case where  $\Delta E_{\text{for}}$  is positive.*

260 To elicit the role of forest and terrestrial  $E$  specifically, each of the four categories is summarized  
 261 for forested land and all land (results shown in Sect. 4.2).

### 262 3 Data

263 For our investigations on moisture recycling, we used the following meteorological data from the  
 264 ERA-Interim (ERA-I) reanalysis at  $1.5^\circ$  resolution provided by the European Centre for Medium  
 265 Range Weather Forecast (ECMWF) (Dee et al., 2011): specific humidity and zonal and  
 266 meridional wind speed at 17 model levels from zero pressure to surface pressure at 6 hours  
 267 resolution, and evaporation and ocean precipitation data at 3 hour resolution. Comparison

268 between ERA-I and MERRA data shows that ERA-I offers good moisture recycling performance  
269 over both South America and Africa (Keys et al., 2014). ERA-I precipitation over Congo is,  
270 however, overestimated as suggested by water balance comparison (Figure S1) with Global  
271 Runoff Data Centre (GRDC) runoff data (Fekete, Vörösmarty, & Grabs, 2002) and shown in  
272 other studies (e.g., Lorenz & Kunstmann, 2011).

273 Thus, the land precipitation used in the moisture recycling analyses were instead taken  
274 from the Multi-Source Weighted-Ensemble Precipitation (MSWEP) v1.1 (Beck et al., 2016) at 3-  
275 hour temporal resolution. The data was originally in 0.25° spatial resolution, and up-scaled to  
276 1.5° by simple aggregation. This precipitation product results from optimally combined  
277 information from two gauge observation based datasets (CPC Unified and GPCC), three satellite  
278 based datasets (CMORPH, GSMaP-MVK, and TMPA 3B42RT), and two reanalysis (ERA-  
279 Interim and JRA-55) datasets. Water balance comparison of effective precipitation (i.e., mean  
280 annual precipitation minus evaporation) with GRDC runoff shown in Fig. S1 indicates that the  
281 precipitation and evaporation products used in this study (Fig. S2a,b) are in agreement with the  
282 runoff data for the Amazon and Congo regions. Mean-years and dry-years dry season anomalies  
283 of precipitation and evaporation are shown in Fig. S3 and S4. All meteorological data  
284 downloaded cover a 36 years period 1979–2014.

285 Land cover data for delineating the Amazon and Congo study regions were taken from the  
286 Land Cover Type Climate Modeling Grid (CMG) MCD12C1 International Geosphere Biosphere  
287 Program (IGBP) land classification created from Terra Moderate Resolution Imaging  
288 Spectroradiometer (MODIS) data (Friedl et al., 2010) for the year 2005.

## 289 4 Results

### 290 4.1 Moisture recycling characteristics

291 The mean annual fraction of forest rainfall that originates from forest moisture sources ( $\rho_{\text{for}}$ ) is  
292 similar between the Amazon (26%) and the Congo (28%) (Table 1), although reliance on  
293 terrestrial moisture sources ( $\rho_{\text{terr}}$ ) is higher in the Congo (64%) than in the Amazon (42%).  
294 Notably, the fraction of forest evaporation that also falls as forest rainfall ( $\varepsilon_{\text{for}}$ ) is higher in the  
295 Amazon (38%) than in the Congo (26%).

296 In dry seasons, rainfall reliance on forest and terrestrial moisture sources (i.e.,  $\rho_{\text{for}}$  and  
297  $\rho_{\text{terr}}$ ) in both regions increase, while the fraction of evaporation that becomes forest rainfall (i.e.,  
298  $\varepsilon_{\text{for}}$ ) decreases. On average, the dry season reliance on forest moisture sources ( $\rho_{\text{for}}$ ) is higher than  
299 the mean annual values by almost 7% in the Amazon (JJAS), 2% in the Congo JF-season and  
300 ~30% in the Congo JJA-season. Dry season reliance on terrestrial sources ( $\rho_{\text{terr}}$ ) is also higher  
301 than the mean annual reliance for both forests: by 13% in the Amazon (JJAS), 8% in Congo JF-  
302 season, and 11% in the Congo JJA-season.

303 In dry years, the dry season reliance on forest moisture further increases by ~4-5% in the  
304 Amazon and Congo, whereas further increase in the reliance on terrestrial sources is slightly  
305 more modest (3% in the Amazon, 1% in the Congo JF-season, and 4% in the Congo JJA-season).  
306 In contrast, a smaller fraction of the dry season forest evaporation becomes forest rainfall ( $\varepsilon_{\text{for}}$ ) in  
307 dry years, both in the Amazon (-16%) and in the Congo (-19% in the JF season, and -9% in the  
308 JJA season). Thus, the forest and terrestrial precipitation recycling ratios are highest, whereas  
309 evaporation recycling ratios are lowest during the dry seasons in dry years across all study  
310 regions.

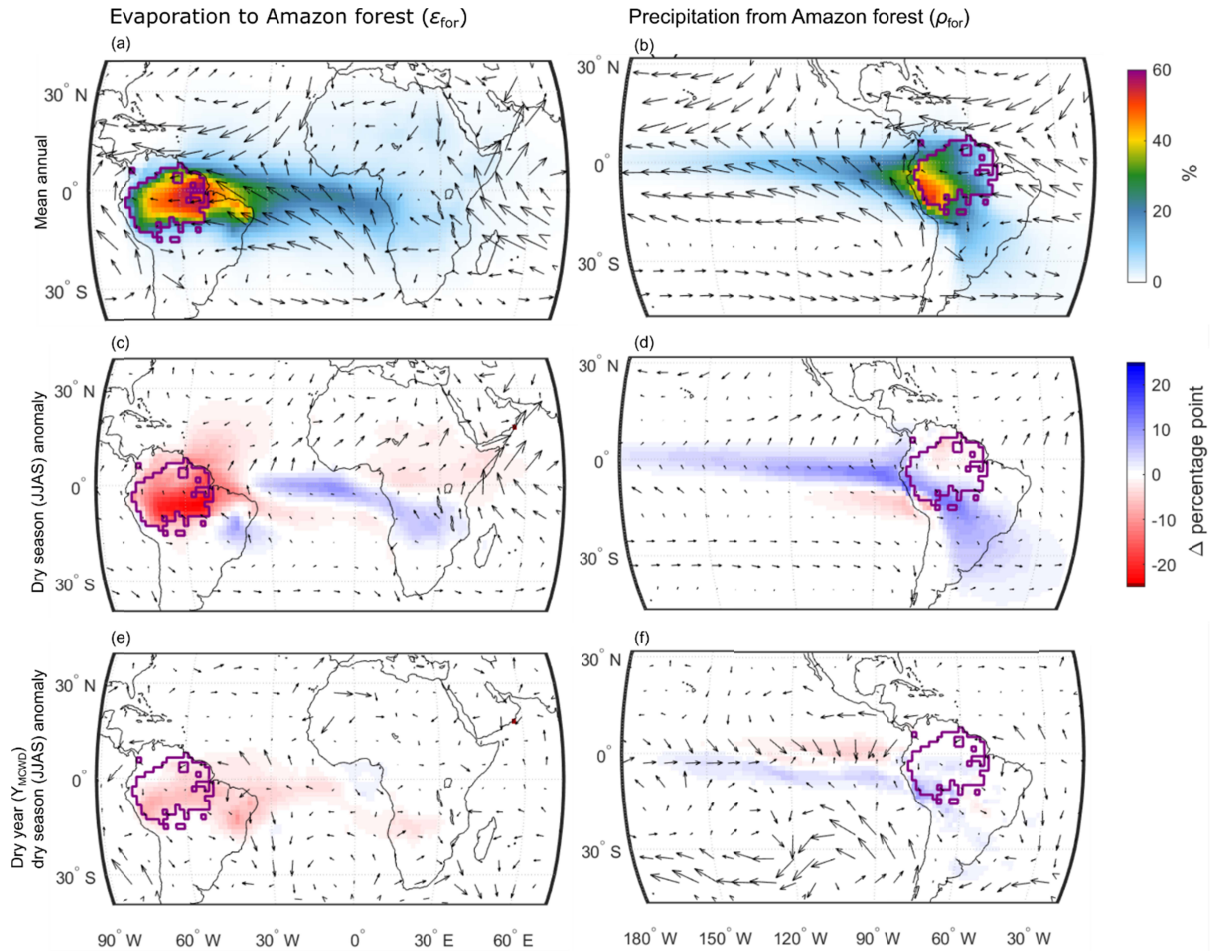
311

312 *Table 1. Overview of moisture recycling metrics in the Amazon and Congo forests. The first*  
 313 *three columns show the percentage of forest rainfall from forest, the percentage of forest rainfall*  
 314 *from land, and the percentage of forest evaporation to forests (i.e., mean  $\rho_{\text{for}}$ ,  $\rho_{\text{terr}}$  and  $\varepsilon_{\text{for}}$  of the*  
 315 *Amazon and Congo rainforests). The last two columns show the relative dry season and dry-year*  
 316 *dry-season anomalies (see definitions in Sect. 2.2.2). The highest value for each recycling ratio*  
 317 *metric is in **bold**.*

Region (dry season months)	Mean recycling ratios ( $\rho$ or $\varepsilon$ , %), see Eq. 3			Mean dry period anomalies				Standard deviation (p.p.)	
	Annual	Dry season	Dry season in dry years	Dry season difference from mean annual, see Eq. 7		Dry-year dry-season difference from mean dry season, see Eq. 8		Seasonal	Dry season inter-annual
				%	p.p.	%	p.p.		
<b><math>\rho_{\text{terr}}</math></b>									
Amazon (JJAS)	42.3	47.6	<b>48.9</b>	12.7	5.4	2.7	1.3	$\pm 5.5$	$\pm 1.6$
Congo (JF)	63.8	68.5	<b>69.0</b>	7.5	4.7	0.71	0.5	$\pm 6.3$	$\pm 4.4$
Congo (JJA)	63.8	70.6	<b>73.2</b>	10.6	6.8	3.8	2.6	$\pm 5.8$	$\pm 3.3$
<b><math>\rho_{\text{for}}</math></b>									
Amazon (JJAS)	26.1	27.9	<b>29.0</b>	6.6	1.7	4.0	1.1	$\pm 3.7$	$\pm 1.9$
Congo (JF)	27.8	28.4	<b>29.8</b>	2.0	0.5	5.0	1.4	$\pm 6.4$	$\pm 3.6$
Congo (JJA)	27.8	36.2	<b>37.8</b>	30.1	8.4	4.5	2.6	$\pm 5.5$	$\pm 3.4$
<b><math>\varepsilon_{\text{for}}</math></b>									
Amazon (JJAS)	<b>38.4</b>	25.0	21.1	-34.9	-13.4	-15.7	-3.9	$\pm 10.3$	$\pm 3.3$
Congo (JF)	<b>26.4</b>	19.2	15.5	-27.2	-7.2	-19.4	-3.7	$\pm 7.2$	$\pm 3.5$
Congo (JJA)	<b>26.4</b>	25.2	23.0	-4.5	-1.2	-9.0	-2.3	$\pm 6.7$	$\pm 3.3$

318





319

320 *Figure 2. The percentage of evaporation destined for the Amazon forest ( $\epsilon_{for}$ ) and percentage of*  
 321 *precipitation originating from the Amazon forest ( $\rho_{for}$ ) at the (a, b) mean annual values, and*  
 322 *their anomalies in the (c, d) dry season (in percentage point difference between the dry season*  
 323 *and the mean annual), and (e, f) dry year (in percentage point difference between the dry season*  
 324 *in dry years and the mean dry season over all years). The arrows represent wind directions in*  
 325 *the lower atmosphere, and the purple lines denote the forest boundaries. For study region and*  
 326 *time period selections, see Sect. 2.1.1 and Table S1, and for moisture recycling metrics*  
 327 *definitions, see Sect. 2.2.2.*

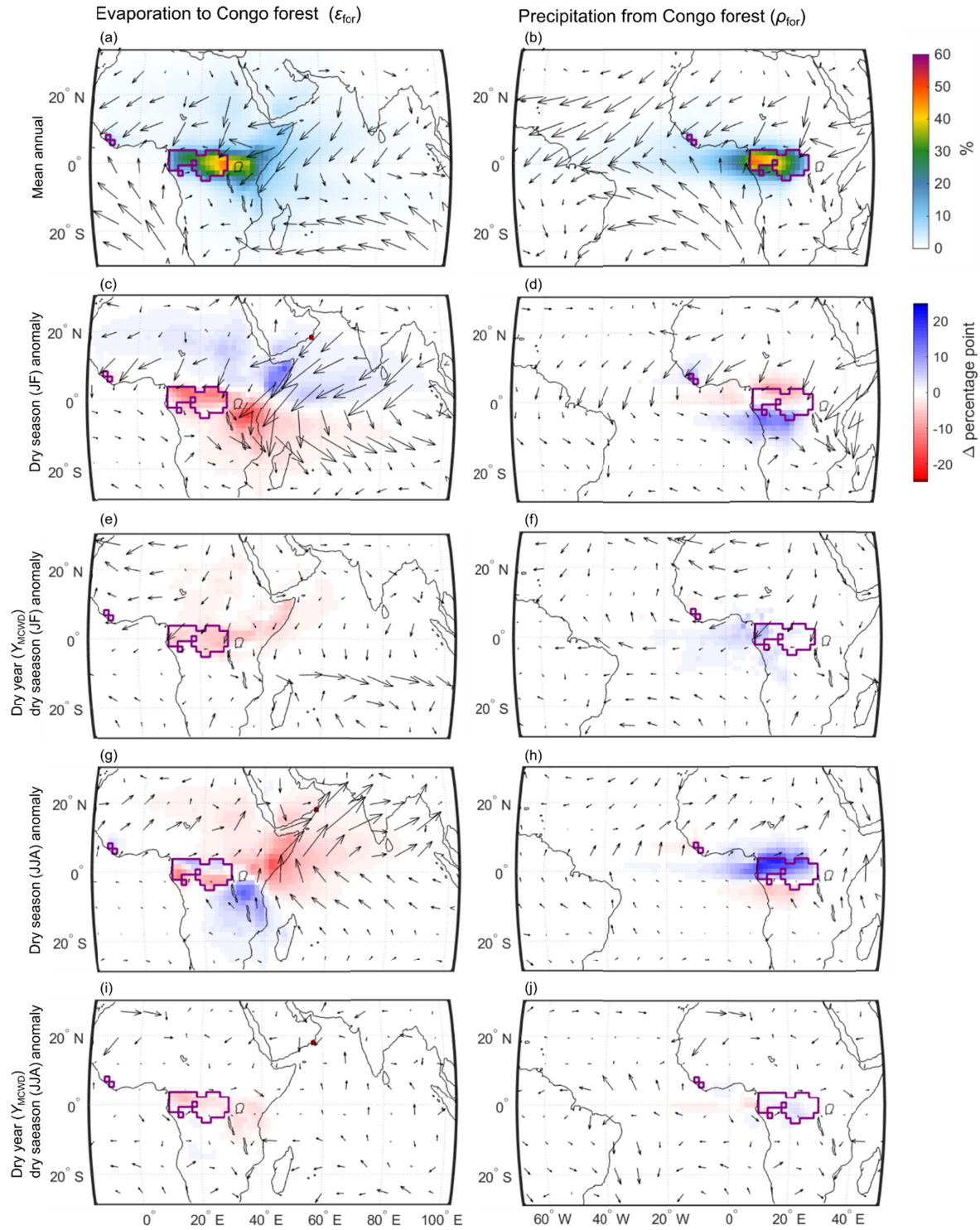
328

329

In the Amazon, the mean annual rainfall reliance on both forest and terrestrial moisture sources is the highest in the southwest (up to  $\sim 50\%$  for  $\rho_{for}$ , see Figure 2b; and  $\sim 60\%$  for  $\rho_{terr}$ , see

330 Fig. S2c). In contrast, the areas where the highest fraction of evaporation recycled within the  
331 forest region are in the east (up to ~60%, Figure 2a). The moisture source for forest moisture  
332 recycling is, thus, concentrated in eastern Amazon, and the moisture sink concentrated in  
333 southwestern Amazon. These patterns follow from wind patterns and are distinctly influenced by  
334 topography. The Andes to the west effectively block east-to-west moisture transport, leading to  
335 particularly high  $\rho_{\text{terr}}$  and  $\rho_{\text{for}}$  along the mountain range. In absolute numbers, similar moisture  
336 recycling patterns are found for  $E_{\text{for}}$  and  $P_{\text{for}}$ , although high values of  $P_{\text{for}}$  are also found in the  
337 northwest where  $\rho_{\text{for}}$  appears to be moderate (compare Figure 2b and Figure S5b).

338         In the Amazon dry season, the relative rainfall reliance on forest moisture ( $\rho_{\text{for}}$ ) is higher  
339 than the mean annual in the southwestern parts (Figure 2d), despite an overall higher absolute  
340 amount of precipitation with forest origin ( $P_{\text{for}}$ ) (Figure S5b). Furthermore, the fraction of dry  
341 season evaporation that falls as rainfall over forests ( $\varepsilon_{\text{for}}$ ) is below the mean annual in almost the  
342 entire forest region (Figure 2c). Instead, there is a higher than mean evaporative contribution  
343 from the equatorial Atlantic Ocean, as well as parts of central Africa and southeastern Brazil  
344 (Figure 2c). In the Amazon dry years (defined in Table S1), the dry season  $\varepsilon_{\text{for}}$  decreases further  
345 across the entire forest region except in the northwest (Figure 2e), whereas the dry season  $\rho_{\text{for}}$   
346 further increases in the southwest (Figure 2f). However, in absolute moisture volumes, both the  
347 dry season  $P$  sources and  $E$  sinks are lower in dry years (Figure S5e,f).



348

349

350

351

*Figure 3. The percentage of evaporation that goes to Congo forest and the percentage of precipitation originating from the Congo forest at the (a, b) mean annual scale, and their absolute anomalies in the (c, d) January-February (JF) dry season (i.e., difference between the*

352 *JF and the mean annual), (e,f) dry year (i.e., between the JF in dry years and the mean JF over*  
353 *all years), (g, h) June-July-August (JJA) dry season (i.e., difference between the JJA and the*  
354 *mean annual), and (i,j) dry year (i.e., between the JJA in dry years and the mean JJA over all*  
355 *years). The arrows represent wind directions in the lower atmosphere, and the purple lines*  
356 *denote the forest boundaries considered as sink and source regions respectively. For study*  
357 *region and time period selections, see Sect.2.2.1, and for moisture recycling metrics definitions,*  
358 *see Sect. 2.2.2.*

359 In the Congo, the mean annual rainfall reliance on both forest and terrestrial moisture  
360 sources is the highest in the west (up to ~50% for  $\rho_{\text{for}}$ , see Figure 3b; and up to ~80% for  $\rho_{\text{terr}}$ ,  
361 see Figure S2c). In contrast, the areas where the highest fraction of evaporation recycled within  
362 the forest region are in the east (up to ~45%, Figure 3a) and the Great Lakes region east of  
363 Congo forest (up to ~40%, Figure 3a). Thus, similarly to the Amazon, the moisture source for  
364 forest moisture recycling is concentrated in the east, and the moisture sink in the west following  
365 predominating wind patterns. In absolute numbers, similar moisture recycling patterns are found  
366 for  $E_{\text{for}}$  and  $P_{\text{for}}$  (Figure S6ab), although high values of  $P_{\text{for}}$  are also found in the central parts  
367 where  $\rho_{\text{for}}$  appears to be moderate (compare Figure 3b and Figure S6b).

368 In the Congo JF season, moisture supply to the Congo forest is higher than the mean  
369 annual in the Horn of Africa and the Indian Ocean ( $\varepsilon_{\text{for}}$  in Figure 3c, and  $E_{\text{for}}$  in Figure S6c).  
370 Note, however, that while the fraction of evaporation in the Horn of Africa that contributes to  
371 forest precipitation ( $\varepsilon_{\text{for}}$ ) is higher during the JF season (Figure 3c), the absolute amounts are  
372 small (Figure S6c). In the northern Congo forest, all forest recycling metrics ( $\varepsilon_{\text{for}}$ ,  $E_{\text{for}}$ ,  $\rho_{\text{for}}$ ,  $P_{\text{for}}$ )  
373 are lower than mean annual during the JF season (Figure 3c, Figure S6c, Figure 3d, Figure S6d).  
374 Nevertheless, the rainfall reliance on forest moisture is higher both in southern parts of the forest

375 and in areas south of the forest ( $\rho_{\text{for}}$  in Figure 3d,  $P_{\text{for}}$  in Figure S6d). Averaged over the forest  
376 region, the JF season  $\varepsilon_{\text{for}}$  is lower (JF: 19%; mean annual: 26%) and  $\rho_{\text{for}}$  is higher (JF: 69%; mean  
377 annual: 64%) than mean annual (Table 1). In dry years, the JF season moisture contribution to  
378 forests ( $\varepsilon_{\text{for}}$ ,  $E_{\text{for}}$ ) further decreases and rainfall reliance on forest moisture ( $\rho_{\text{for}}$ ,  $P_{\text{for}}$ ) further  
379 increases in the Congo forest region (Figure 3e,f, Figure S6e,f, Table 1).

380 In the Congo JJA season, the spatial patterns of moisture recycling anomalies are almost  
381 the opposite of the JF season anomalies, due to a reversal of the predominant wind directions  
382 associated with the seasonal shifts of the Inter-Tropical Convergence Zone (Figure 3c,d,g,h, and  
383 S6c,d,g,h). For instance, moisture supply to the Congo forest, which was higher than the mean  
384 annual in the JF season, is instead lower than the mean annual in the JJA season in the Horn of  
385 Africa and the Indian Ocean ( $\varepsilon_{\text{for}}$  in Figure 3g, and  $E_{\text{for}}$  in Figure S6g). Similarly, the  
386 precipitation recycling anomaly metrics are reversed between the JF and JJA seasons, and forest  
387 rainfall reliance on forest moisture is notably higher than average in the northern parts the forest  
388 in the JJA season (locally up to  $\sim 20$  percentage points higher than mean annual, see Figure 3h  
389 and S6h)). In the dry years, slightly less evaporation in the western parts of the forest contributes  
390 to forest rainfall (Figure 3i, S6i), while slightly more forest rainfall in southern parts of Congo  
391 originates from the forest itself (Figure 3j, S6j).

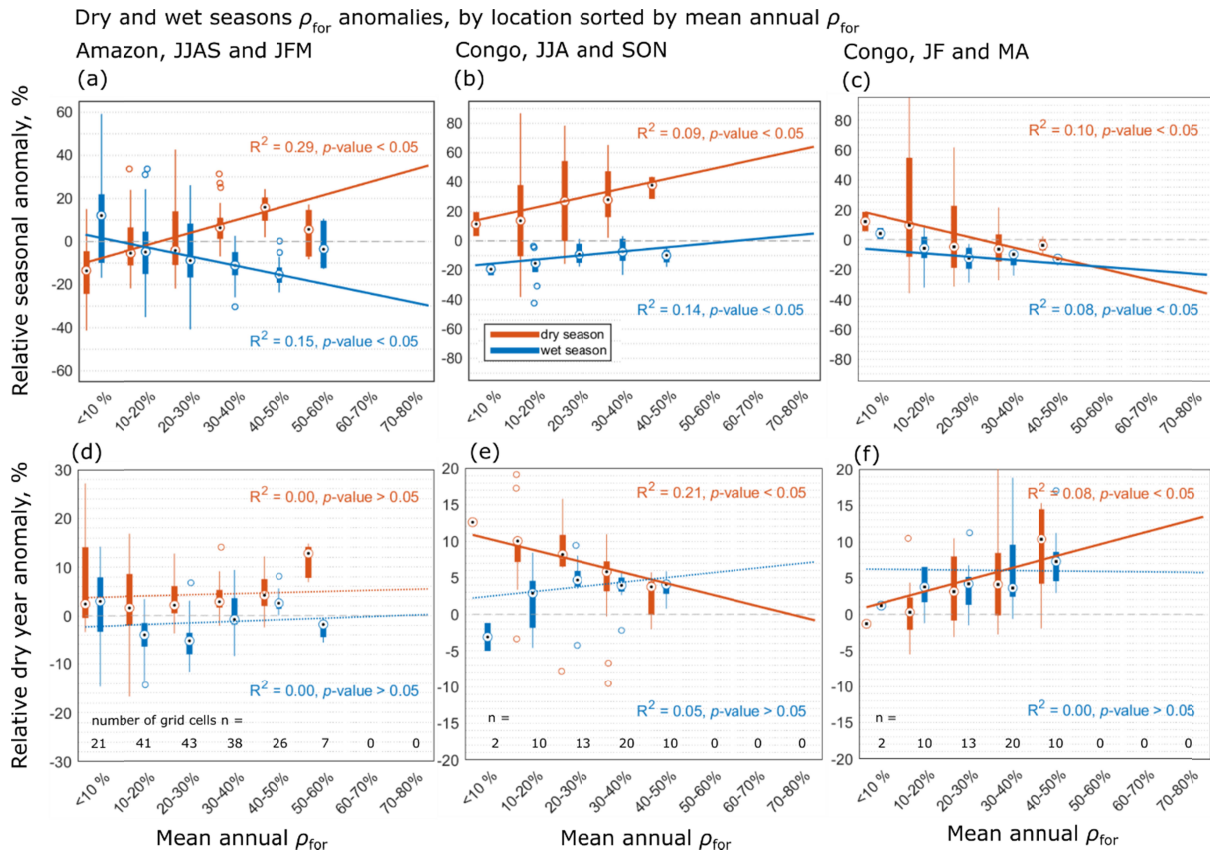
#### 392 4.2 Dry season amplification stronger in areas with high mean annual forest precipitation 393 recycling

394 Across both the Amazon and Congo, the JJAS and JJA dry seasons tend to see higher anomalies  
395 of rainfall self-reliance in areas with high mean  $\rho_{\text{for}}$  (Figure 4ab). In Congo's dry JF season,  
396 however, dry season  $\rho_{\text{for}}$  anomalies tend to be lower in areas with lower mean annual  $\rho_{\text{for}}$  (see  
397 Figure 4c). Notably, the boreal summer dry season anomalies of  $\rho_{\text{for}}$  in the Amazon and Congo

398 tend to be distinctly different from those of the wet seasons. The wet season  $\rho_{for}$  anomalies in the  
 399 Amazon and the wet MA season anomalies in the Congo are not only negative, but also decrease  
 400 with increasing mean annual  $\rho_{for}$  (Figure 4abc). In the Congo,  $\rho_{for}$  anomalies in the wet season  
 401 (SON) are generally negative, but tend to be higher in areas with higher mean annual  $\rho_{for}$  (Figure  
 402 4b).

403 In the dry years, the differences between dry and wet seasons anomalies increase (Figure  
 404 4def). The dry-year dry-season anomalies tend to be positive, but lower in areas with high mean  
 405  $\rho_{for}$ . In contrast, the dry-year wet-seasons anomalies tend to be negative and increase with  
 406 increasing mean annual  $\rho_{for}$ .

407



408

409 *Figure 4. Relationships between seasonal anomalies of forest self-reliance ( $\rho_{for}$  in the Amazon*  
 410 *and Congo forests, respectively) and mean annual  $\rho_{for}$  (a,d) the Amazon and (b,c,e,f) Congo. For*

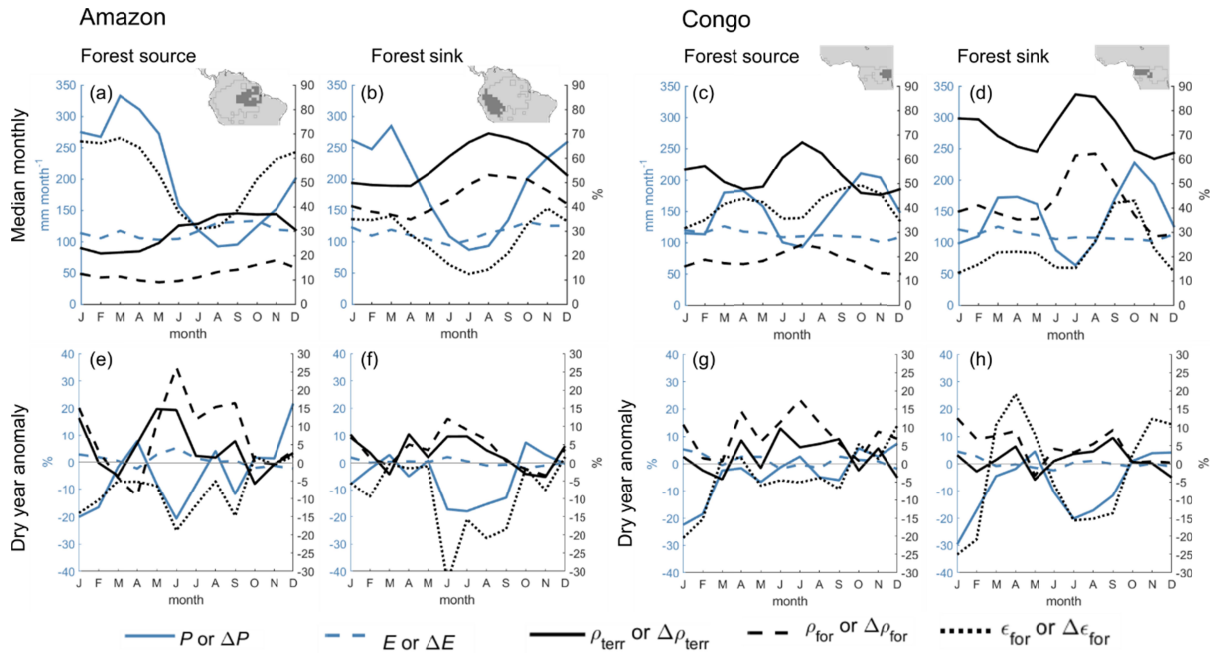
411 *study region and time period selections, see Sect. 2.2.1, and for moisture recycling metrics*  
412 *definitions, see Sect. 2.2.2.*

#### 413 4.3 Climatology and trends in forest moisture source and sink regions

414 Monthly  $P$  and  $\rho_{\text{terr}}$  vary strongly with seasons (Figure 5a-d) in the Amazon and Congo forests,  
415 whereas forest  $\varepsilon_{\text{for}}$  and  $\rho_{\text{for}}$  tend to vary less, and forest  $E$  remain stable throughout the year.  
416 Overall, when  $P$  and  $\varepsilon_{\text{for}}$  are at their lowest in the dry seasons, whereas  $\rho_{\text{terr}}$  and  $\rho_{\text{for}}$  have the  
417 reversed seasonality and peak in dry seasons.

418 In the Amazon forest source hotspot (i.e., the 25% of the forest areas with the highest  
419 values of  $\varepsilon_{\text{for}}$ ), the median  $\varepsilon_{\text{for}}$  varies between 70% in March and 30% in July, while  $\rho_{\text{for}}$  remain  
420 below 20% throughout the year (Figure 5a). In the Amazon forest sink hotspot (i.e., the 25% of  
421 the forest areas with the highest values of  $\rho_{\text{for}}$ ), the median  $\varepsilon_{\text{for}}$  varies between 40% in  
422 March/November and almost 10% in July, while  $\rho_{\text{for}}$  reaches 55% in the dry season and its value  
423 never drops below 35% (Figure 5b). Throughout the year, the Amazon sink  $\rho_{\text{for}}$  is about 10-15  
424 percentage points lower than  $\rho_{\text{terr}}$  ( $\rho_{\text{terr}}$ : 50-70 %, and  $\rho_{\text{for}}$  : 35-55 %) (Figure 5b).

425 In the Congo source hotspot, the median  $\varepsilon_{\text{for}}$  varies between 50% in October and 30% in  
426 January, while  $\rho_{\text{for}}$  peaks at 25% in July (Figure 5c). In the Congo forest sink hotspot,  $\rho_{\text{for}}$  peaks  
427 most distinctly in the JJA season at 62% and never drops below 30%, whereas  $\varepsilon_{\text{for}}$  peaks at 45%  
428 in September and October and largely remains below 20-30%. In both the source and sink  
429 hotspots,  $\rho_{\text{for}}$  has one distinct peak in the JJA season, whereas  $\rho_{\text{terr}}$  peaks twice: once in the JF  
430 season and once in the JJA season. Because of this, the difference between  $\rho_{\text{for}}$  and  $\rho_{\text{terr}}$  is  
431 smallest in the JJA season (about 25-30 percentage point), when  $\rho_{\text{terr}}$  exceeds 85%.



432

433

434

435

436

437

438

439

440

441

442

443

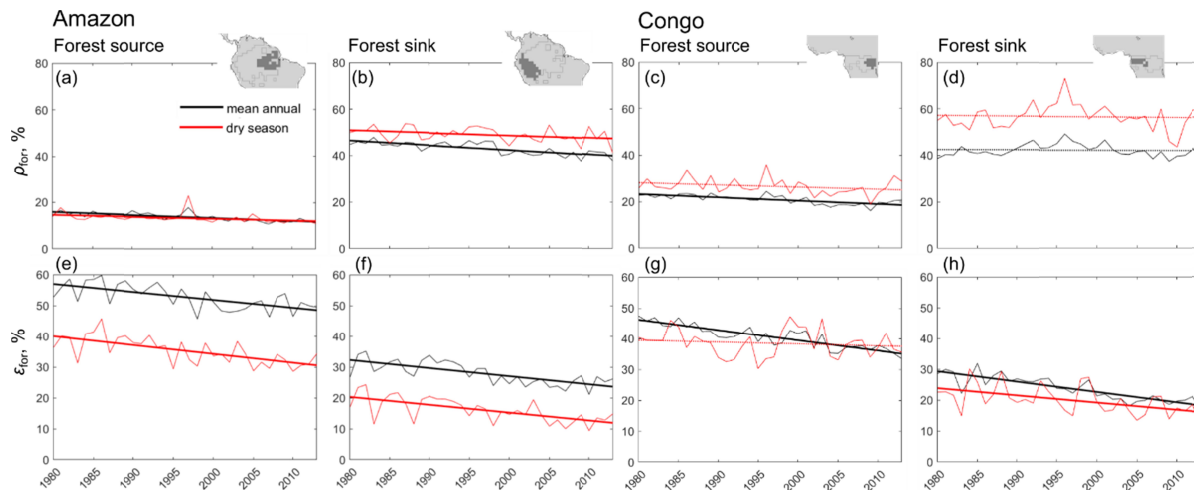
444

445

*Figure 5. Monthly variations in precipitation ( $P$ , blue solid line), evaporation ( $E$ , blue dashed line), percentage of precipitation from land ( $\rho_{terr}$ , black solid line), percentage of precipitation from forest ( $\rho_{for}$ , black dashed line), percentage of evaporation to forest ( $\epsilon_{for}$ , black dotted line), and their dry year anomalies over the study period 1980-2013 for the source and sink hotspots (dark grey in maps) in (a,b,e,f) Amazon and (c,d,g,h) Congo. The anomalies (e,f,g,h) are given as the mean dry year values relative to median values of all years. For study region and time period selections, see Sect. 2.2.1, and for moisture recycling metrics definitions, see Sect. 2.2.2.*

The dry years anomalies (Figure 5e,f,g,h) do not have a consistent seasonal pattern. Only the Amazon forest has precipitation considerably lower than mean annual in the JJAS dry season, when also  $\rho_{for}$  and  $\rho_{terr}$  are higher than mean annual (up to 10% in the sink and up to 25% in the source hotspot) (Figure 5e,f). In the Congo forest, dry years increase only the relative role of moisture supply from forests: only  $\rho_{for}$  is increased in both hotspots by up to 10-15% in the dry season, whereas  $\rho_{terr}$  increases remain below 5% (Figure 5g,h).





446

447 *Figure 6. Trends in the percentage of rainfall from forest ( $\rho_{for}$ ) and of evaporation contributing*  
 448 *to forest rainfall ( $\epsilon_{for}$ ) in Amazon and Congo source and sink hotspot regions. Significant ( $p$ -*  
 449 *value  $< 0.05$ ) linear trends in solid lines and non-significant trends are shown with dashed lines*  
 450 *(i.e., dry season trend lines in c and g, and both mean annual and dry season trend lines in d).*

451 In the Amazon forest, there has been a weak decrease over time in the fraction of rainfall reliance  
 452 on forest moisture sources ( $\rho_{for}$ ) (Figure 6ab) and a strong decrease in the fraction of forest  
 453 evaporation that returns as rainfall over forest areas ( $\epsilon_{for}$ ) (Figure 6ef). The decrease in dry season  
 454  $\rho_{for}$  in the Amazon sink hotspot is, however, considerably weaker than the decrease in mean  
 455 annual  $\rho_{for}$ , contributing to an upward trend in dry season  $\rho_{for}$  anomaly. In absolute volumes, dry  
 456 season anomaly in forest rainfall self-reliance has not changed significantly (Figure S7), while  
 457 total mean annual  $P$  has increased and dry season  $P$  has stagnated (Figure S8). Although  $E$  in the  
 458 Amazon forest has also increased, less  $E$  precipitates over the forest (Figure S7) and more of the  
 459 increase in  $P$  originates from elsewhere.

460 In the Congo forest, no strong and significant trends could be observed for  $\rho_{for}$ . The  
 461 downward trend for mean annual  $\epsilon_{for}$  is, however, strong and significant in both Congo source  
 462 and sink hotspots. Because the downward trend for dry season  $\epsilon_{for}$  is weaker than the trend for

463 mean annual  $\varepsilon_{\text{for}}$ , there is a downward trend in dry season  $\varepsilon_{\text{for}}$  anomaly. Also in absolute volumes,  
464 dry season anomaly in forest evaporation contribution to its own rainfall ( $E_{\text{for}}$ ) decreased in both  
465 Congo source and sink hotspots (Figure S7), even though the increase in mean annual  $E$  has  
466 exceeded the increase in dry season  $E$  (Figure S8).

#### 467 4.4 Correspondence and contrariety between $E_{\text{for}}$ and $E$ anomalies

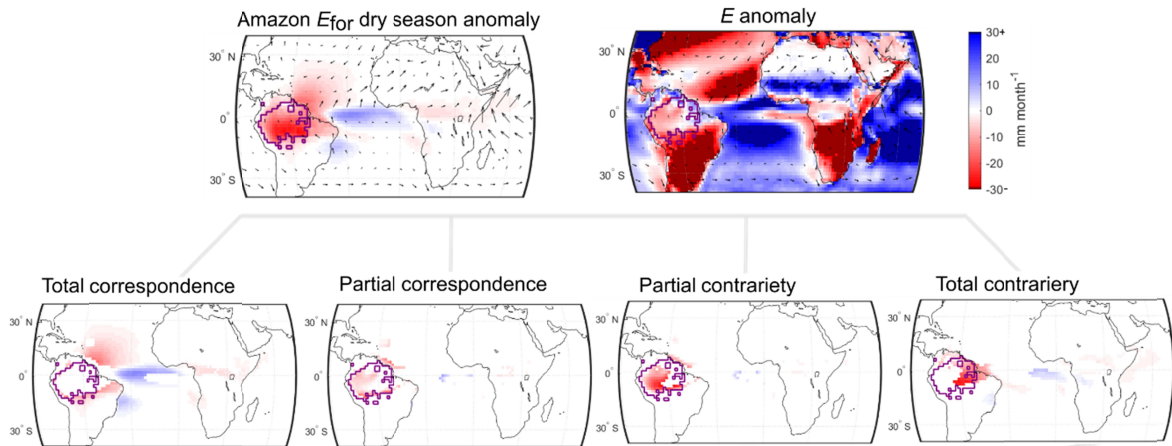
468 To explore the role of forest  $E$  in supplying moisture to forest  $P$  during dry periods, we compare  
469 the forest  $E_{\text{for}}$  and  $E$  anomalies (where  $E_{\text{for}}$  is the evaporation that precipitates in areas with forest  
470 cover  $> 85\%$ , and thus by mass conservation, the sum of  $E_{\text{for}}$  is equivalent to total forest  $P$ ).  
471 Correspondence between  $E_{\text{for}}$  and  $E$  can indicate that the  $E$  anomaly drives and supports the  $E_{\text{for}}$   
472 anomaly, whereas contrariety can indicate that the  $E$  anomaly acts to dampen the  $E_{\text{for}}$  anomaly.  
473 In other words, in case of contrariety,  $E_{\text{for}}$  anomalies are driven by wind changes and occur  
474 despite  $E$  anomalies of opposite sign (see Sect. 2.2.3 for methods description).

475         Dry-season and dry-year dry-season rainfall anomalies in both the Amazon and Congo  
476 are driven by  $E$  anomalies external to the rainforests, with almost no correspondence between  
477 forest  $E$  and  $E_{\text{for}}$ . In the Amazon, correspondence between dry season  $E$  anomalies and  $E_{\text{for}}$   
478 anomalies mainly occurs in the Atlantic Ocean, whereas contrariety mainly occurs in the  
479 Amazon forest (Figure 7a). This highlights the role of the forest for buffering the negative  $E_{\text{for}}$   
480 anomaly. Summing up the fraction of the contrariety over forest, other land, and oceans  
481 separately shows that forest is the largest contributor to contrarieties in negative JJAS  $E_{\text{for}}$   
482 anomaly (Figure 7b). We further note that the forest contribution to the negative anomaly  
483 contrariety has increased significantly over time, while its contribution to negative anomaly  
484 correspondence has remained low (Figure S9ad). In terms of negative dry year anomaly, forest

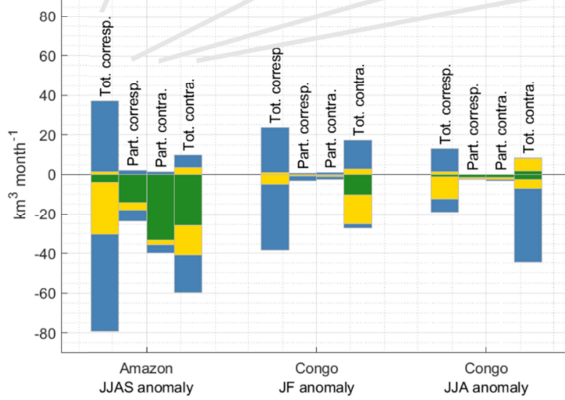
485 contrariety also sums up to more than a third of the total contrarities (Figure 7c), mainly in the  
486 southern parts of the Amazon (Figure S10g).

487 In the Congo,  $E$  anomaly in forests and other land areas contradicts negative  $E_{\text{for}}$  anomaly  
488 in the JF dry season (Figure 7b,c). In the JJA season, however, land  $E$  appears to contribute to  
489 both the positive and negative  $E_{\text{for}}$  anomaly (Figure 7b), whereas ocean  $E$  anomaly contradict  
490 both negative dry season and dry year  $E_{\text{for}}$  anomaly (Figure 7b,c). The role of forests for negative  
491 dry season anomaly contributions and contrarities has not changed as drastically as in the  
492 Amazon (Figure S9b,c,e,f). In the JJA dry season, forests have rather decreased their buffering of  
493 negative contrariety over time (Figure S9f). For spatial breakdown of the correspondence and  
494 contrariety components in Congo, see Fig. S11 and S12.

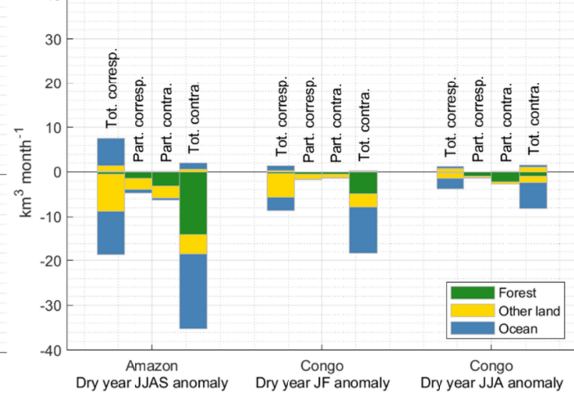
(a) Spatial example of  $E_{\text{for}}$  and  $E$  anomaly correspondence and contrariety



(b) Correspondence of dry season anomaly



(c) Correspondence of dry year anomaly in dry season



495

496 *Figure 7. Breakdown of forest precipitation anomalies into its causes: correspondence ( $E_{\text{for}}$  and*

497  *$E$  anomalies agree in sign) and contrariety ( $E_{\text{for}}$  and  $E$  anomalies have opposite signs). (a)*

498 *Spatial breakdown of the different components for the Amazon JJAS-mean  $E_{\text{for}}$  anomaly. The*

499 *spatially distributed categories consist of forest, other land, and ocean for both Amazon and*

500 *Congo for the (b) dry season anomalies, and (c) dry-years dry-season anomalies. Calculations*

501 *are explained in Sect. 2.2.3.*

502 **4.5 Dry season amplification of countries' forest moisture reliance**

503 Countries' reliance on rainforest moisture during dry seasons can differ considerably from their

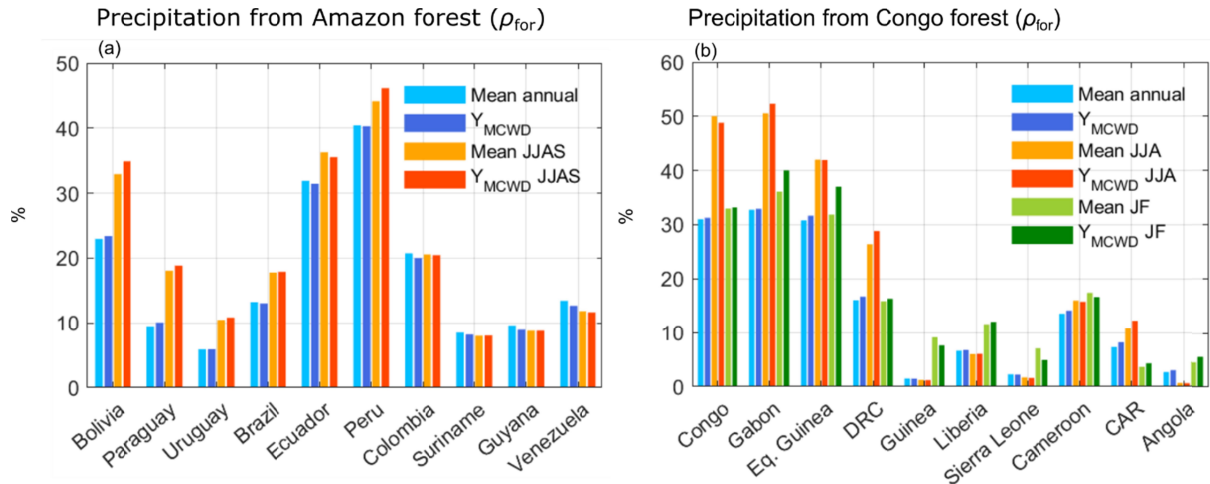
504 mean annual reliance (Figure 8a,b). The biggest absolute differences between country-scale

505 mean annual and dry season  $\rho_{\text{for}}$  in South America are found in Bolivia, Paraguay, Uruguay,  
506 Brazil, Ecuador, and Peru (in the order of declining difference, Figure 8a). For example, Bolivia  
507 depends on the forest for 23% of its mean annual precipitation, but 35% of its dry year JJAS  
508 precipitation; and Paraguay doubles its forest moisture reliance going from 9% at mean annual  
509 scale to 19% during the JJAS season in dry years.

510 In Africa, the biggest dry season anomalies are found in Congo, Gabon, Equatorial  
511 Guinea, Democratic Republic of Congo, Guinea, Liberia, Sierra Leone, Cameroon, CAR, and  
512 Angola (in the order of declining difference, Figure 8b). For example, both Congo and Gabon  
513 receives around a third of their mean annual precipitation from the rainforest, but around half of  
514 their precipitation during the JJA dry season originates as forest moisture. In Guinea and Sierra  
515 Leone,  $\rho_{\text{for}}$  is negligibly low (1-2%) at a mean annual scale, but considerable during the dry  
516 seasons (7-9%).

517 Furthermore, the countries that host the largest areas of rainforests are not necessarily the  
518 countries that are most dependent on rainforest moisture supply for their rainfall, due to the  
519 forest's upwind positions. In South America, the country that hosts the largest rainforest areas is  
520 Brazil. However, Peru, Ecuador, Bolivia, Colombia, and Venezuela have a higher mean annual  
521 rainfall reliance on the Amazon forest than Brazil. In the dry season and dry years, Paraguayan  
522 precipitation has a similar forest moisture reliance as that of Brazil (Figure 8a). Similarly, in  
523 Africa, the Democratic Republic of Congo (DRC) is less dependent on the Congo rainforest for  
524 its precipitation than Gabon, Congo, and Equatorial Guinea, despite hosting the largest area of  
525 forest (Figure 8b).

526



527

528 *Figure 8. Percentage of country-level precipitation coming from a) Amazon and b) Congo forest*529 *evaporation. Ten countries are shown in the order of declining maximum difference between*530 *mean annual and dry season  $\rho_{for}$ . CAR stands for the Central African Republic, and DRC stands*531 *for the Democratic Republic of Congo.*532 **5 Discussion**533 **5.1 Amplification of forest precipitation recycling during dry periods**

534 We examined the mean year and dry year dry season anomalies of moisture sources and sinks of

535 forest  $P$  and  $E$  in the Amazon and Congo region based on 34 years of data and simulations. We

536 selected the driest periods in the rainforests in order to understand moisture recycling variability

537 when it is most critical for forest mortality and resilience. We find that forest precipitation

538 recycling during dry seasons amplifies and increases the ratio of forest  $P$  originating from forest539  $E$  in both the Amazon and Congo. This relative seasonal increase in forest precipitation recycling

540 increases further in dry years.

541 We found that the dry period forest rainfall dependency increases more in the Congo than

542 in the Amazon, and is substantially more important than the amplification of moisture supply

543 from other terrestrial sources. In the Amazon, the relative moisture contribution from both  
544 terrestrial areas and the forest increases during the dry season (i.e., 13% increase in  $\rho_{\text{terr}}$  and 7%  
545 in  $\rho_{\text{for}}$ ), and increases further by 3-4% in dry years (Table 1). In the Congo, both the dry season  
546 (JJA) and the dry year amplification is substantially larger for moisture sources from the forest  
547 itself than from terrestrial sources in general (see Sect. 4.1).

548 Furthermore, we found that the relative dry season anomaly of  $\rho_{\text{terr}}$  and  $\rho_{\text{for}}$  (Amazon and  
549 Congo boreal summer, but not Congo JF dry season) tends to be *higher* in regions with high  
550 mean annual  $\rho_{\text{terr}}$  and  $\rho_{\text{for}}$ , while the dry year dry season anomalies tend to be *lower* in regions  
551 with high mean annual  $\rho_{\text{terr}}$  and  $\rho_{\text{for}}$  (see Sect. 4.2). Both mean-years dry-season and dry-year  
552 dry-season anomalies are, however, largely positive across the forest region. In other words,  
553 forest areas that have a generally high reliance on their own moisture supply for rainfall tend to  
554 increase that dependence more than other forest regions during dry seasons. In dry years, the  
555 positive anomalies further increase, but less than in forest areas with lower mean annual  $\rho_{\text{terr}}$  and  
556  $\rho_{\text{for}}$ .

557 The dry season anomalies in rainfall self-reliance are likely to continue to be relevant  
558 given current trends. In the Amazon forest, the dry season anomaly of rainfall self-reliance has  
559 increased in the Amazon sink hotspot, because dry season  $\rho_{\text{for}}$  declined less than mean annual  
560  $\rho_{\text{for}}$ , possibly partly because overall dry season precipitation has not increased during the study  
561 period. Under future climate, global models project that recycling ratios over the Amazon and  
562 Congo basin will decline (Baker & Spracklen, 2022; Findell et al., 2019). However, it is unclear  
563 if this will affect the role of forest supply under for example increased severity, frequency, and  
564 duration of droughts, or increase in dry season length (Khanna, Medvigy, Fueglistaler, & Walko,  
565 2017; Marengo et al., 2011). Dry season forest supply will also depend on the overall effects of a

566 variety of forest responses (e.g., mortality, rooting depth adaptation) to environmental stressors  
567 that are not well captured in climate models (Schewe et al., 2019). In the Congo forest, rainfall  
568 self-reliance does not show any significant trend, but has more interannual variability than in the  
569 Amazon (Figure 6).

570 Our estimates of increases in forest rainfall self-reliance during dry season and dry years  
571 in the Amazon compares well with many others studies (Table S2). For example, Zemp et al.  
572 (2014) similarly found 1-2 percentage point increase in the precipitation recycling ratio in the  
573 Amazon basin during the dry seasons compared to the mean annual, and a weak 1 percentage  
574 point weakening in precipitation recycling was found by Chug, Dominguez, & Yang, (2022).  
575 Others found more considerable amplification of precipitation recycling. For example, Staal et  
576 al. (2018) found an increase of ~10 percentage point increase, in 2005 and 2010 during the dry  
577 season in northwestern Amazon. Bagley et al. (2014) found a 7 percentage point increase in dry  
578 season Amazon rainfall self-reliance during the 2005 and 2010 drought years in comparison to  
579 wet years, similar to e.g., findings of Mu, Biggs, & De Sales (2021). However, our findings  
580 differ considerably from the conclusions of Satyamurty et al., (2013), who found recycling to be  
581 lower in dry seasons. Their recycling estimate assumed that any moisture that is not converged  
582 constitutes recycled precipitation, although in reality, the outgoing flux may comprise both  
583 locally evaporated moisture and atmospheric water passing through. Thus, their estimates  
584 constitute an upper limit to recycling that is not directly comparable to ours. Our study also  
585 suffers from limitations, such as a relatively coarse spatial resolution and use of only two  
586 atmospheric layers, which does not allow us to capture smaller-scale atmospheric circulation.  
587 Future studies could also consider analyzing the dry season for different parts of the Amazon



588 forests separately, as e.g., parts of the northern Amazon have the opposite seasonality than that  
589 of the rest of the Amazon (Fisch et al., 2004).

590 Differences in study region selection are likely another major cause of discrepancy when  
591 comparing among studies (see Table S2), more so in the Congo region due to the considerable  
592 mismatch in the extent of the Congo rainforest extent and the Congo basin. Depending on region  
593 selection and methods, mean annual  $\rho_{\text{for}}$  vary between 28% and 68% in different studies (see  
594 Table S2; e.g., Dyer et al., (2017); te Wierik, Keune, Miralles, & Gupta, (2022)). For example,  
595 Sorí et al. (2017)'s analysis of the Congo river basin found that internal basin precipitation  
596 recycling decreases in dry seasons and dry years despite increases in evaporation. However,  
597 Pokam et al., (2012), who analyzed moisture recycling over a study region better approximating  
598 the forest region, arrived at a conclusion more similar to ours: that precipitation recycling ratio  
599 increases in the dry season. This sensitivity of precipitation recycling estimates to study region  
600 selection in Central Africa may be attributable to both heterogeneity in land-cover type, and  
601 seasonal shifts in circulation patterns modulated by a latitudinal gradient in sea surface  
602 temperature in the Indian Ocean (Dyer et al., 2017).

## 603 5.2 High forest evaporation rates help explain dry period increase in $\rho_{\text{for}}$

604 We conclude that high dry period forest evaporation has an important role in increasing dry  
605 period  $\rho_{\text{for}}$ . In Sect. 4.2, we found that forest rainfall self-reliance occurs despite decreases in  $\varepsilon_{\text{for}}$ ,  
606 i.e., the fraction of forest  $E$  that returns as forest  $P$ . This seemingly paradoxical situation arises  
607 because  $\varepsilon_{\text{for}}$  decrease comparatively less during a dry period (Sect. 4.3) and the drastic dry period  
608 decrease in  $P$  is compensated and counter-acted by increasing or unchanging forest  $E$  as it is  
609 energy-limited rather than water limited (Baker et al. 2021). The same response was found  
610 during the onset of the Western European drought in 2018, where initially evaporation was also

611 not water limited (Al Hasan, Link, & van der Ent, 2021; Benedict et al., 2021). The enhanced  
612 role of forest evaporation during dry season can also be due to a higher sensitivity of  
613 precipitation to atmospheric moisture content change below certain levels (Baudena et al., 2021).  
614 In Sect. 4.4, we explicitly compared the dry period anomalies of  $E_{\text{for}}$  and  $E$ , and found that  $E$   
615 anomalies in forests and other terrestrial areas dominate the contrariety with negative dry period  
616 anomalies  $E_{\text{for}}$  in the Amazon and Congo boreal summer dry seasons. In other words, positive  $E$   
617 dry period anomalies in forests and other terrestrial areas act to dampen negative, wind-driven  
618  $E_{\text{for}}$  anomalies. This indicates that high dry period forest  $E$  rates, in fact, *counteract* wind-driven  
619 anomalies to support dry period increase in  $\rho_{\text{for}}$ .

620 The anomaly correspondence-contrariety analysis method introduced here differentiates  
621 how  $E$  anomalies contribute to the amplification or dampening of  $E_{\text{for}}$  anomalies. Future  
622 applications of the method could, for example, shed light on the role of  $E$  anomalies for  $E_{\text{for}}$   
623 anomalies during heatwaves, under climate change, or land cover change, as an addition to  
624 current methods such as correlation analyses (O'Connor et al., 2021; Pranindita, Wang-  
625 Erlandsson, Fetzer, & Teuling, 2022) and coupled model simulations under different scenarios  
626 (Swann, Longo, Knox, Lee, & Moorcroft, 2015). In addition, distributed or lumped versions of  
627  $E_{\text{for}}$  and  $E$  anomaly correspondence and contrariety also help highlight the need to understand  
628 both  $P$  source and  $E$  sink, as one-sided analyses of  $P$  source are unable to explain the respective  
629 role of  $E$  and wind anomalies in driving anomalies in moisture source reliance.

### 630 5.3 Potential implications for forest governance

631 Increasingly, policies to promote nature-based solutions to address climate change such as forest  
632 restoration and conservation are being proposed, planned and implemented (Chaplin-Kramer et  
633 al., 2019; Griscom et al., 2017). The benefit of forest moisture supply for forest resilience,

634 agriculture, and water resources are increasingly recognized (Cui et al., 2022; Hoek van Dijke et  
635 al., 2022; Leite-Filho et al., 2021). At the same time, dry season length in both the Amazon and  
636 Congo forests is increasing (Fu et al., 2013; Jiang et al., 2019) and rainforests are becoming  
637 increasingly vulnerable to repeated droughts (Tao et al., 2022). Thus, it will be important to  
638 understand where measures to prevent deforestation or promote forestation might have the  
639 greatest benefits for counteracting such drying trends (Obbe A. Tuinenburg, Bosmans, & Staal,  
640 2022). In Congo, the dependency of forest rainfall on terrestrial evaporation ( $\rho_{\text{terr}}$  is 64%, and  
641 ~70% in dry seasons) is much higher than the dependence on forest evaporation ( $\rho_{\text{for}}$  is 28%, and  
642 ~30-40% in dry seasons), indicating that substantial land areas without dense forests are also  
643 important for moisture supply to rainfall. Such differences are also found in the Amazon,  
644 although differences are smaller (at the mean annual scale,  $\rho_{\text{for}} = 26\%$ ,  $\rho_{\text{terr}} = 42\%$ ). Compared to  
645 the Amazon, the Congo rainforest is also projected to face greater future threats of forest loss and  
646 greater deforestation impacts on regional precipitation (Smith, Baker, & Spracklen, 2023).

647         The need for governance of moisture flows is increasingly being discussed in the  
648 scientific literature (Keys, Wang-Erlandsson, Gordon, Galaz, & Ebbesson, 2017; te Wierik,  
649 Gupta, Cammeraat, & Artzy-Randrup, 2020). Hitherto, most analyses of moisture flows at the  
650 country scale focus on the mean annual scale (Dirmeyer, Brubaker, & DelSole, 2009; Keys et al.,  
651 2017). Here, the analyses (Sect. 4.5) show that dry period amplification of forest moisture  
652 reliance can be very high. For example, in the case of Guinea and Sierra Leone, countries'  
653 rainfall reliance on forest moisture grow from negligible (1-2%) at the mean annual scale to  
654 substantial (7-9%) in the dry season. This means that the consideration of forests' importance for  
655 different nations' management and governance contexts will need to go beyond the mean annual  
656 scale and account for seasonal variations.

657 **6 Conclusions**

658 To conclude, we found an increase in the role of forest evaporation for buffering against forest  
659 rainfall reductions during dry seasons and further during dry years. High dry period forest  
660 evaporation enables forests to rely on their own moisture supply for rainfall, despite a decreasing  
661 fraction of forest evaporation that contributes to forest rainfall. In the forest areas with the  
662 highest reliance on forest moisture supply, dry season amplifications of forest precipitation  
663 recycling ratios tend to be larger than elsewhere. We conclude that dry period amplification of  
664 precipitation recycling ratios highlights additional risks of loss of forest resilience from  
665 deforestation as well as opportunities in resilience building from forest conservation and  
666 restoration. As such, accounting for an enhanced forest rainfall self-reliance in dry periods can be  
667 essential for understanding the combined impact of deforestation and climate change on forest  
668 resilience.

669 **Acknowledgments**

670 We would like to thank Prof. Hubert Savenije for valuable discussions during research  
671 design and useful comments on the manuscript. L.W.-E. and L.J.G. acknowledge support from  
672 Formas (Project “Ripples of Resilience”, 2018-02345) and from the Swedish Research Council  
673 (Project “Beyond Forest-Rainfall myths”, 2014-1224). LWE further acknowledges funding from  
674 the Japan Society for the Promotion of Science (JSPS) postdoctoral fellowship (ID: P-17761),  
675 Formas (Project “Governing atmospheric water flows”, 2019-01220) and the IKEA Foundation.  
676 AS acknowledges support from the Talent Programme grant VI.Veni.202.170 by the Dutch  
677 Research Council (NWO). LWE, IF, and AS were further supported by the European Research  
678 Council, (Project Earth Resilience in the Anthropocene, the ERC-2016-ADG 743080).

679

680 **Open Research**

681 The ERA-Interim reanalyses data used in this study can be downloaded at  
682 <https://www.ecmwf.int/en/forecasts/datasets/reanalysis-datasets/era-interim>. Precipitation data  
683 from MSWEP can be obtained here: <http://www.gloh2o.org/mswep/>. The corresponding WAM-  
684 2layers code in Python is available at <https://github.com/ruudvdent/WAM2layersPython>. The  
685 data of tracked precipitation and evaporation of the forest regions in this study are downloadable  
686 at <https://doi.org/10.5281/zenodo.7635445>.

687

688

689 **References**

- 690 Al Hasan, F., Link, A., & van der Ent, R. J. (2021). The effect of water vapor originating from land on the 2018  
691 drought development in europe. *Water (Switzerland)*, 13(20), 2856. <https://doi.org/10.3390/W13202856/S1>
- 692 Angelini, I. M., Garstang, M., Davis, R. E., Hayden, B., Fitzjarrald, D. R., Legates, D. R., ... Connors, V. (2011). On the  
693 coupling between vegetation and the atmosphere. *Theoretical and Applied Climatology*, 105(1–2), 243–261.  
694 <https://doi.org/10.1007/s00704-010-0377-5>
- 695 Bagley, J. E., Desai, A. R., Harding, K. J., Snyder, P. K., & Foley, J. a. (2014). Drought and Deforestation: Has land  
696 cover change influenced recent precipitation extremes in the Amazon? *Journal of Climate*, 27, 345–361.  
697 <https://doi.org/10.1175/JCLI-D-12-00369.1>
- 698 Baker, J. C. A., & Spracklen, D. V. (2022). Divergent representation of precipitation recycling in the Amazon and the  
699 Congo in CMIP6 models. *Geophysical Research Abstracts*, 49, e2021GL095136.  
700 <https://doi.org/10.1029/2021GL095136>
- 701 Baudena, M., Tuinenburg, O. A., Ferdinand, P. A., & Staal, A. (2021). Effects of land- -use change in the Amazon on  
702 precipitation are likely underestimated. *Global Change Biology*, 27(July), 5580–5587.  
703 <https://doi.org/10.1111/gcb.15810>
- 704 Beck, H. E., Van Dijk, A. I. J. M., Levizzani, V., Schellekens, J., Miralles, D. G., Martens, B., & de Roo, A. (2016).

- 705 MSWEP: 3-hourly 0.25° global gridded precipitation (1979–2015). *Hydrology and Earth System Sciences*  
706 *Discussions*, 1–38. <https://doi.org/10.5194/hess-2016-236>
- 707 Benedict, I., van Heerwaarden, C. C., van der Linden, E. C., Weerts, A. H., & Hazeleger, W. (2021). Anomalous  
708 moisture sources of the Rhine basin during the extremely dry summers of 2003 and 2018. *Weather and*  
709 *Climate Extremes*, 31, 100302. <https://doi.org/10.1016/J.WACE.2020.100302>
- 710 Boulton, C. A., Lenton, T. M., & Boers, N. (2022). Pronounced loss of Amazon rainforest resilience since the early  
711 2000s. *Nature Climate Change*, 12(3), 271–278. <https://doi.org/10.1038/s41558-022-01287-8>
- 712 Burde, G. I., Gandush, C., & Bayarjargal, Y. (2006). Bulk recycling models with incomplete vertical mixing. Part II:  
713 Precipitation recycling in the Amazon basin. *Journal of Climate*, 19(8), 1473–1489. Retrieved from  
714 <http://www.scopus.com/inward/record.url?eid=2-s2.0-33646794416&partnerID=40>
- 715 Chaplin-Kramer, R., Sharp, R. P., Weil, C., Bennett, E. M., Pascual, U., Arkema, K. K., ... Daily, G. C. (2019). Global  
716 modeling of nature’s contributions to people. *Science*, 366(6462). <https://doi.org/10.1126/science.aaw3372>
- 717 Chug, D., Dominguez, F., & Yang, Z. (2022). The Amazon and La Plata River Basins as Moisture Sources of South  
718 America: Climatology and Intraseasonal Variability. *Journal of Geophysical Research: Atmospheres*, 127(12),  
719 e2021JD035455. <https://doi.org/10.1029/2021JD035455>
- 720 Costa, M. H., Biajoli, M. C., Sanches, L., Malhado, A. C. M., Hutyra, L. R., Da Rocha, H. R., ... De Araújo, A. C. (2010).  
721 Atmospheric versus vegetation controls of Amazonian tropical rain forest evapotranspiration: Are the wet  
722 and seasonally dry rain forests any different? *Journal of Geophysical Research: Biogeosciences*, 115(4), 1–9.  
723 <https://doi.org/10.1029/2009JG001179>
- 724 Cui, J., Lian, X., Huntingford, C., Gimeno, L., Wang, T., Ding, J., ... Piao, S. (2022). Global water availability boosted  
725 by vegetation-driven changes in atmospheric moisture transport. *Nature Geoscience* 2022 15:12, 15(12),  
726 982–988. <https://doi.org/10.1038/s41561-022-01061-7>
- 727 Dai, A. (2013). Increasing drought under global warming in observations and models. *Nature Climate Change*, 3(1),  
728 52–58. <https://doi.org/10.1038/nclimate1633>
- 729 Dee, D., Uppala, S., Simmons, A. J., Berrisford, P., Poli, P., Kobayashi, S., ... Vitart, F. (2011). The ERA-Interim  
730 reanalysis: configuration and performance of the data assimilation system. *Quarterly Journal of the Royal*  
731 *Meteorological Society*, 137, 553–597. <https://doi.org/10.1002/qj.828>

- 732 Dirmeyer, P. A., Brubaker, K. L., & DelSole, T. (2009). Import and export of atmospheric water vapor between  
733 nations. *Journal of Hydrology*, 365(1–2), 11–22. <https://doi.org/10.1016/j.jhydrol.2008.11.016>
- 734 Dominguez, F., Eiras-Barca, J., Yang, Z., Bock, D., Nieto, R., & Gimeno, L. (2022). Amazonian Moisture Recycling  
735 Revisited Using WRF With Water Vapor Tracers. *JGR Atmospheres*, 127(4), e2021JD035259.
- 736 Duffy, P. B., Brando, P., Asner, G. P., & Field, C. B. (2015). Projections of future meteorological drought and wet  
737 periods in the Amazon. *Proceedings of the National Academy of Sciences of the United States of America*,  
738 112(43), 13172–13177. <https://doi.org/10.1073/pnas.1421010112>
- 739 Dyer, E. L. E., Jones, D. B. A., Nusbaumer, J., Li, H., Collins, O., Vettoretti, G., & Noone, D. (2017). Congo Basin  
740 precipitation: Assessing seasonality, regional interactions, and sources of moisture. *Journal of Geophysical*  
741 *Research: Atmospheres*, 122(13), 6882–6898. <https://doi.org/10.1002/2016JD026240>
- 742 Eltahir, E. A. B., & Bras, R. L. (1994). Precipitation recycling in the Amazon Basin. *Quarterly Journal of the Royal*  
743 *Meteorological Society*, 120(518), 861–880. Retrieved from  
744 <http://www.scopus.com/inward/record.url?eid=2-s2.0-0028581801&partnerID=40>
- 745 Fekete, B. M., Vörösmarty, C. J., & Grabs, W. (2002). High-resolution fields of global runoff combining observed  
746 river discharge and simulated water balances. *Global Biogeochemical Cycles*, 16(3), 15-1-15–10.  
747 <https://doi.org/10.1029/1999GB001254>
- 748 Findell, K. L., Keys, P. W., van der Ent, R. J., Lintner, B. R., Berg, A., Krasting, J. P., ... Krasting, J. P. (2019). Rising  
749 Temperatures Increase Importance of Oceanic Evaporation as a Source for Continental Precipitation. *Journal*  
750 *of Climate*, 32(22), 7713–7726. <https://doi.org/10.1175/JCLI-D-19-0145.1>
- 751 Fisch, G., Tota, J., Machado, L. A. T., Silva Dias, M. A. F., da, R. F., Nobre, C. A., ... Gash, J. H. C. (2004). The  
752 convective boundary layer over pasture and forest in Amazonia. *Theoretical and Applied Climatology*, 78(1–  
753 3), 47–59. <https://doi.org/10.1007/s00704-004-0043-x>
- 754 Forzieri, G., Dakos, V., Mcdowell, N. G., Ramdane, A., & Cescatti, A. (2022). *Emerging signals of declining forest*  
755 *resilience under climate change*. 608(August). <https://doi.org/10.1038/s41586-022-04959-9>
- 756 Friedl, M. a., Sulla-Menashe, D., Tan, B., Schneider, A., Ramankutty, N., Sibley, A., & Huang, X. (2010). MODIS  
757 Collection 5 global land cover: Algorithm refinements and characterization of new datasets. *Remote Sensing*  
758 *of Environment*, 114(1), 168–182. <https://doi.org/10.1016/j.rse.2009.08.016>

- 759 Fu, R., Yin, L., Li, W., Arias, P. A., Dickinson, R. E., Huang, L., ... Myneni, R. B. (2013). Increased dry-season length  
760 over southern Amazonia in recent decades and its implication for future climate projection. *Proceedings of*  
761 *the National Academy of Sciences of the United States of America*, *110*(45), 18110–18115.  
762 <https://doi.org/10.1073/pnas.1302584110>
- 763 Greene, C. A., Thirumalai, K., Kearney, K. A., Delgado, J. M., Schwanghart, W., Wolfenbarger, N. S., ... Blankenship,  
764 D. D. (2019). The Climate Data Toolbox for MATLAB. *Geochemistry, Geophysics, Geosystems*, *20*(7), 3774–  
765 3781. <https://doi.org/10.1029/2019GC008392>
- 766 Griscom, B. W., Adams, J., Ellis, P. W., Houghton, R. A., Lomax, G., Miteva, D. A., ... Fargione, J. (2017). Natural  
767 climate solutions. *Proceedings of the National Academy of Sciences of the United States of America*, *114*(44),  
768 11645–11650. <https://doi.org/10.1073/pnas.1710465114>
- 769 Hirota, M., Holmgren, M., van Nes, E. H., & Scheffer, M. (2011). Global resilience of tropical forest and savanna to  
770 critical transitions. *Science*, *334*(6053), 232–235. <https://doi.org/10.1126/science.1210657>
- 771 Hoek van Dijke, A. J., Herold, M., Mallick, K., Benedict, I., Machwitz, M., Schlerf, M., ... Teuling, A. J. (2022). Shifts in  
772 regional water availability due to global tree restoration. *Nature Geoscience* *2022* *15*:5, *15*(5), 363–368.  
773 <https://doi.org/10.1038/s41561-022-00935-0>
- 774 Hubau, W., Lewis, S. L., Phillips, O. L., Affum-Baffoe, K., Beeckman, H., Cuní-Sanchez, A., ... Zemagho, L. (2020).  
775 Asynchronous carbon sink saturation in African and Amazonian tropical forests. *Nature*, *579*(7797), 80–87.  
776 <https://doi.org/10.1038/s41586-020-2035-0>
- 777 Jiang, Y., Zhou, L., Tucker, C. J., Raghavendra, A., Hua, W., Liu, Y. Y., & Joiner, J. (2019). Widespread increase of  
778 boreal summer dry season length over the Congo rainforest. *Nature Climate Change*, *9*(August), 617–62.  
779 <https://doi.org/10.1038/s41558-019-0512-y>
- 780 Keys, P. W., Barnes, E. A., van der Ent, R. J., & Gordon, L. J. (2014). Variability of moisture recycling using a  
781 precipitationshed framework. *Hydrology and Earth System Sciences*, *18*(10), 3937–3950.  
782 <https://doi.org/10.5194/hess-18-3937-2014>
- 783 Keys, P. W., van der Ent, R. J., Gordon, L. J., Hoff, H., Nikoli, R., & Savenije, H. H. G. (2012). Analyzing  
784 precipitationsheds to understand the vulnerability of rainfall dependent regions. *Biogeosciences*, *9*(2), 733–  
785 746. <https://doi.org/10.5194/bg-9-733-2012>



- 786 Keys, P. W., Wang-Erlandsson, L., Gordon, L. J., Galaz, V., & Ebbesson, J. (2017). Approaching moisture recycling  
787 governance. *Global Environmental Change*, 45. <https://doi.org/10.1016/j.gloenvcha.2017.04.007>
- 788 Khanna, J., Medvigy, D., Fueglistaler, S., & Walko, R. (2017). Regional dry-season climate changes due to three  
789 decades of Amazonian deforestation. *Nature Climate Change*, 7(3), 200–204.  
790 <https://doi.org/10.1038/nclimate3226>
- 791 Leite-Filho, A. T., Soares-filho, B. S., Davis, J. L., Abrahão, G. M., & Börner, J. (2021). Deforestation reduces rainfall  
792 and agricultural revenues in the Brazilian Amazon. *Nature Communications*, 12(2591).  
793 <https://doi.org/10.1038/s41467-021-22840-7>
- 794 Lewis, S. L., Brando, P. M., Phillips, O. L., Heijden, G. M. F. Van Der, & Nepstad, D. (2010). *The 2010 Amazon*  
795 *Drought*. (Ci), 2010.
- 796 Lewis, S. L., Edwards, D. P., & Galbraith, D. (2015). Increasing human dominance of tropical forests. *Science*,  
797 349(6250), 827–832. <https://doi.org/10.1126/science.aaa9932>
- 798 Link, A., van der Ent, R., Berger, M., Eisner, S., & Finkbeiner, M. (2020). The fate of land evaporation – a global  
799 dataset. *Earth Syst. Sci. Data*, 12(3), 1897–1912.
- 800 Lorenz, C., & Kunstmann, H. (2011). The Hydrological Cycle in Three State-of-the-Art Reanalyses: Intercomparison  
801 and Performance Analysis. *Journal of Hydrometeorology*, submitted(5), 1397–1420.  
802 <https://doi.org/10.1175/JHM-D-11-088.1>
- 803 Malhi, Y., Aragão, L. E. O. C., Galbraith, D., Huntingford, C., Fisher, R., Zelazowski, P., ... Meir, P. (2009). Exploring  
804 the likelihood and mechanism of a climate-change-induced dieback of the Amazon rainforest. *Proceedings of*  
805 *the National Academy of Sciences of the United States of America*, 106(49), 20610–20615.  
806 <https://doi.org/10.1073/pnas.0804619106>
- 807 Malhi, Y., Gardner, T. A., Goldsmith, G. R., Silman, M. R., & Zelazowski, P. (2014). Tropical forests in the  
808 anthropocene. *Annual Review of Environment and Resources*, 39(August), 125–159.  
809 <https://doi.org/10.1146/annurev-environ-030713-155141>
- 810 Marengo, J. A., Tomasella, J., Alves, L. M., Soares, W. R., & Rodriguez, D. A. (2011). The drought of 2010 in the  
811 context of historical droughts in the Amazon region. *Geophysical Research Letters*, 38(12), 1–5.  
812 <https://doi.org/10.1029/2011GL047436>

- 813 Miralles, D. G., Brutsaert, W., Dolman, A. J., & Gash, J. H. (2020). *On the Use of the Term “ Evapotranspiration ”*  
814 *Water Resources Research*. <https://doi.org/10.1029/2020WR028055>
- 815 Mitchard, E. T. A. (2018). The tropical forest carbon cycle and climate change. *Nature*, *559*(7715), 527–534.  
816 <https://doi.org/10.1038/s41586-018-0300-2>
- 817 Mu, Y., Biggs, T. W., & De Sales, F. (2021). Forests Mitigate Drought in an Agricultural Region of the Brazilian  
818 Amazon: Atmospheric Moisture Tracking to Identify Critical Source Areas. *Geophysical Research Letters*,  
819 *48*(5). <https://doi.org/10.1029/2020GL091380>
- 820 Nascimento, M. G. do, Herdies, D. L., & De Souza, D. O. (2016). The south American water balance: The influence of  
821 low-level jets. *Journal of Climate*, *29*(4), 1429–1449. <https://doi.org/10.1175/JCLI-D-15-0065.1>
- 822 O’Connor, J. C., Dekker, S. C., Staal, A., Tuinenburg, O. A., Rebel, K. T., & Santos, M. J. (2021). Forests buffer against  
823 variations in precipitation. *Global Change Biology*, *27*(19), 4686–4696. <https://doi.org/10.1111/gcb.15763>
- 824 Pimm, S. L., Jenkins, C. N., Abell, R., Brooks, T. M., Gittleman, J. L., Joppa, L. N., ... Sexton, J. O. (2014). The  
825 biodiversity of species and their rates of extinction, distribution, and protection. *Science (New York, N.Y.)*,  
826 *344*(6187), 1246752. <https://doi.org/10.1126/science.1246752>
- 827 Pokam, W. M., Djotang, L. A. T., & Mkankam, F. K. (2012). Atmospheric water vapor transport and recycling in  
828 Equatorial Central Africa through NCEP/NCAR reanalysis data. *Climate Dynamics*, *38*(9–10), 1715–1729.  
829 <https://doi.org/10.1007/s00382-011-1242-7>
- 830 Pranindita, A., Wang-Erlandsson, L., Fetzer, I., & Teuling, A. J. (2022). Moisture recycling and the potential role of  
831 forests as moisture source during European heatwaves. *Climate Dynamics*, *58*(1–2), 609–624.  
832 <https://doi.org/10.1007/s00382-021-05921-7>
- 833 Satyamurty, P., da Costa, C. P. W., & Manzi, A. O. (2013). Moisture source for the Amazon Basin: a study of  
834 contrasting years. *Theoretical and Applied Climatology*, *111*(1–2), 195–209. [https://doi.org/10.1007/s00704-](https://doi.org/10.1007/s00704-012-0637-7)  
835 [012-0637-7](https://doi.org/10.1007/s00704-012-0637-7)
- 836 Schewe, J., Gosling, S. N., Reyser, C., Zhao, F., Ciais, P., Elliott, J., ... Warszawski, L. (2019). State-of-the-art global  
837 models underestimate impacts from climate extremes. *Nature Communications* *2019 10:1*, *10*(1), 1–14.  
838 <https://doi.org/10.1038/s41467-019-08745-6>
- 839 Silva Junior, C. H. L., Pessôa, A. C. M., Carvalho, N. S., Reis, J. B. C., Anderson, L. O., & Aragão, L. E. O. C. (2021). The

- 840 Brazilian Amazon deforestation rate in 2020 is the greatest of the decade. *Nature Ecology and Evolution*,  
841 5(2), 144–145. <https://doi.org/10.1038/s41559-020-01368-x>
- 842 Singh, C., van der Ent, R., Wang-Erlandsson, L., & Fetzer, I. (2022). Hydroclimatic adaptation critical to the resilience  
843 of tropical forests. *Global Change Biology*, 28(9), 2930–2939. <https://doi.org/10.1111/GCB.16115>
- 844 Smith, C., Baker, J. C. A., & Spracklen, D. V. (2023). Tropical deforestation causes large reductions in observed  
845 precipitation. *Nature*, 615(March). <https://doi.org/10.1038/s41586-022-05690-1>
- 846 Sorí, R., Nieto, R., Vicente-Serrano, S. M., Drumond, A., & Gimeno, L. (2017). A Lagrangian perspective of the  
847 hydrological cycle in the Congo River basin. *Earth Syst. Dynam*, 8(3), 653–675. [https://doi.org/10.5194/esd-8-](https://doi.org/10.5194/esd-8-653-2017)  
848 653-2017
- 849 Spracklen, D. V., Arnold, S. R., & Taylor, C. M. (2012). Observations of increased tropical rainfall preceded by air  
850 passage over forests. *Nature*, 489(7415), 282–285. <https://doi.org/10.1038/nature11390>
- 851 Spracklen, D. V., & Garcia-Carreras, L. (2015). The impact of Amazonian deforestation on Amazon basin rainfall.  
852 *Geophysical Research Letters*, 42, 9546–9552. <https://doi.org/10.1002/2015GL066063>
- 853 Staal, A., Flores, B. M., Aguiar, A. P. D., Bosmans, J. H. C., Fetzer, I., & Tuinenburg, O. A. (2020). *Feedback between*  
854 *drought and deforestation in the Amazon*.
- 855 Staal, A., Tuinenburg, O. A., Bosmans, J. H. C., Holmgren, M., Van Nes, E. H., Scheffer, M., ... Dekker, S. C. (2018).  
856 Forest-rainfall cascades buffer against drought across the Amazon. *Nature Climate Change*, 8(6), 539–543.  
857 <https://doi.org/10.1038/s41558-018-0177-y>
- 858 Staver, A. C., Archibald, S., & Levin, S. A. (2011). The Global Extent and Determinants of Savanna and Forest as  
859 Alternative Biome States. *Science*, 334(6053), 230–232. <https://doi.org/10.1126/science.1210465>
- 860 Swann, A. L. S., Longo, M., Knox, R. G., Lee, E., & Moorcroft, P. R. (2015). Future deforestation in the Amazon and  
861 consequences for South American climate. *Agricultural and Forest Meteorology*, 214–215, 12–24.  
862 <https://doi.org/10.1016/j.agrformet.2015.07.006>
- 863 Tao, S., Chave, J., Frison, P.-L., Toan, T. Le, Ciais, P., Fang, J., ... Saatchi, S. (2022). Increasing and widespread  
864 vulnerability of intact tropical rainforests to repeated droughts. *PNAS*, 119(37), e2116626119. Retrieved  
865 from <https://doi.org/10.1073/pnas.2116626119>
- 866 Tchatchou, B., Sonwa, D. J., Anne, S. I., & Tiani, M. (2015). Deforestation and forest degradation in the Congo

- 867 Basin: state of knowledge, current causes and perspectives. In *Deforestation et degradation des forets dans*  
868 *le Bassin du Congo: etat des lieux, causes actuelles et perspectives*. <https://doi.org/10.17528/cifor/005894>
- 869 te Wierik, S. A., Gupta, J., Cammeraat, E. L. H., & Artzy-Randrup, Y. A. (2020). The need for green and atmospheric  
870 water governance. *WIREs Water*, 7(2). <https://doi.org/10.1002/wat2.1406>
- 871 te Wierik, S. A., Keune, J., Miralles, D. G., & Gupta, J. (2022). The contribution of transpiration to precipitation over  
872 African watersheds. *Water Resources Research*, 58, e2021WR031721.  
873 <https://doi.org/10.1029/2021WR031721>
- 874 Tuinenburg, O. A., & Staal, A. (2020). Tracking the global flows of atmospheric moisture and associated  
875 uncertainties. *Hydrol. Earth Syst. Sci.*, (24), 2419–2435. <https://doi.org/10.5194/hess-2019-597>
- 876 Tuinenburg, Obbe A., Bosmans, J. H. C., & Staal, A. (2022). The global potential of forest restoration for drought  
877 mitigation. *Environmental Research Letters*, 17(3), 034045. <https://doi.org/10.1088/1748-9326/AC55B8>
- 878 van der Ent, R. J., Savenije, H. G. G., Schaefli, B., & Steele-Dunne, S. C. (2010). Origin and fate of atmospheric  
879 moisture over continents. *Water Resources Research*, 46(9), 1–12. <https://doi.org/10.1029/2010WR009127>
- 880 van der Ent, R. J., & Tuinenburg, O. A. (2017). The residence time of water in the atmosphere revisited. *Hydrology*  
881 *and Earth System Sciences*, 21(2), 779–790. <https://doi.org/10.5194/hess-21-779-2017>
- 882 van der Ent, R. J., Tuinenburg, O. A., Knoche, H. R., Kunstmann, H., & Savenije, H. H. G. (2013). Should we use a  
883 simple or complex model for moisture recycling and atmospheric moisture tracking? *Hydrology and Earth*  
884 *System Sciences*, 17(12), 4869–4884. <https://doi.org/10.5194/hess-17-4869-2013>
- 885 van der Ent, R. J., Wang-Erlandsson, L., Keys, P. W., & Savenije, H. H. G. (2014). Contrasting roles of interception  
886 and transpiration in the hydrological cycle – Part 2: Moisture recycling. *Earth System Dynamics*, 5(2), 471–  
887 489. <https://doi.org/10.5194/esd-5-471-2014>
- 888 Williamson, G. B., Laurance, W. F., Oliveira, A. A., Delamônica, P., Gascon, C., Lovejoy, T. E., & Pohl, L. (2000).  
889 Amazonian Tree Mortality during the 1997 El Niño Drought. *Conservation Biology*, 14(5), 1538–1542.  
890 <https://doi.org/10.1046/j.1523-1739.2000.99298.x>
- 891 Worden, S., Fu, R., Chakraborty, S., Liu, J., & Worden, J. (2021). Where Does Moisture Come From Over the Congo  
892 Basin? *JGR Biogeosciences*, 126(8), e2020JG006024.
- 893 Wunderling, N., Staal, A., Sakschewski, B., Hirota, M., Tuinenburg, O. A., Donges, J. F., ... Winkelmann, R. (2022).

894 Recurrent droughts increase risk of cascading tipping events by outpacing adaptive capacities in the Amazon  
895 rainforest. *PNAS*, 119(32), e2120777119. <https://doi.org/10.1073/pnas.2120777119/-/DCSupplemental>

896 Xiao, M., & Cui, Y. (2021). Source of Evaporation for the Seasonal Precipitation in the Pearl River Delta, China.  
897 *Water Resources Research*, 57(8), e2020WR028564. <https://doi.org/10.1029/2020WR028564>

898 Zemp, D. C., Schleussner, C.-F., Barbosa, H. M. J., Hirota, M., Montade, V., Sampaio, G., ... Rammig, A. (2017). Self-  
899 amplified Amazon forest loss due to vegetation-atmosphere feedbacks. *Nature Communications*, 8, 14681.  
900 <https://doi.org/10.1038/ncomms14681>

901 Zemp, D. C., Schleussner, C.-F., Barbosa, H. M. J., van der Ent, R. J., Donges, J. F., Heinke, J., ... Rammig, a. (2014).  
902 On the importance of cascading moisture recycling in South America. *Atmospheric Chemistry and Physics*,  
903 14(23), 13337–13359. <https://doi.org/10.5194/acp-14-13337-2014>

904 Zhou, L., Tian, Y., Myneni, R. B., Ciais, P., Saatchi, S., Liu, Y. Y., ... Hwang, T. (2014). Widespread decline of Congo  
905 rainforest greenness in the past decade. *Nature*, 509(7498), 86–90. <https://doi.org/10.1038/nature13265>

906

907

908